이학박사학위논문

Polyplex-Stability Enhancement by Hydrophobic Modification of PAM-DET Dendrimer and Dermal Gene Delivery Application of PAMAM-Arg Dendrimer

소수성 물질로 치환된 PAM-DET 에 의한 폴리플렉스의 안정도 향상과 경피 유전자 전달을 위한 PAMAM-Arg 의 응용

2013년 2월

서울대학교 대학원

화학부 생화학전공

정 윤 성

Polyplex-Stability Enhancement by Hydrophobic Modification of PAM-DET Dendrimer and Dermal Gene Delivery Application of PAMAM-Arg Dendrimer

지도교수 박 종 상

이 논문을 이학박사 학위논문으로 제출함

2012년 12월

서울대학교 대학원

화학부 생화학전공

정 윤 성

정윤성의 이학박사 학위논문을 인준함

2012년 12월

위 원 장 이 연 (인)

부위원장 박 종 상 (인)

위 원 최 준 식 (인)

위 원 임 흥 배 (인)

위 원 김 태 일 (인)

Polyplex-Stability Enhancement by Hydrophobic Modification of PAM-DET Dendrimer and Dermal Gene Delivery Application of PAMAM-Arg Dendrimer

By Yunseong Jeong

Supervisor: Professor Jong-Sang Park

A Thesis Submitted to the Graduated Faculty of

Seoul National University in Partial Fulfillment of

the Requirement for the Degree of Doctor of Philosophy

February 2012

Table of Contents

Contents ……..…….....iii

General Introduction …….....…..……...….....v

List of Publication ……..……..……..…….....viii

List of Tables…….....…….....……x

List of Figures…….....…..……....……xi

Part A. Effect of Hydrophobic Group Conjugation on Stability of pDNA / Polyamidoamine-diethylentriamine (PAM-DET) Polyplex against Ionic Strength

1. Abstract 1

2. Introduction 2

3. Materials and Methods 5

4. Results and Discussion 11

5. Conclusions 16

6. References 17

Part B. Application of Polyamidoamine-Arginine (PAMAM-R) to Mouse Skin as a Method of Gene Delivery

1. Abstract 45

2. Introduction 46

3. Materials and Methods 48

4. Results and Discussion 54

5. Conclusions 55

6. References 56

Abstract in Korean (국문초록) 66

General Introduction

Various medical and pharmacological studies have been conducted to identify nano-scale therapeutic methods, and nano-sized therapy via gene-delivery systems has gained attention over the last 25 years. In this regard, gene-delivery carriers that show remarkable properties and outstanding gene-delivery potential have been studied, and several forms of these carriers have been developed, including liposomes, nano-particles, and gene-polymer complexes. Dendrimers, a group of nonviral gene-delivery carriers, are polymers with highly branched structures, globular shapes, well-defined molecular weights, and functionalized end groups. A number of modifications and functionalizations of dendrimers have been attempted by many researchers in order to solve the general problem associated with these structures, i.e., the high cytotoxicity of polymers such as the 25-kDa poly(ethylenimine) (PEI) and polyamidoamine dendrimer (PAMAM). As a result of these attempts, PAMAM-R and PAM-DET, which are respectively arginine- and diethyltriamine (DETA)-modified PAMAM dendrimers, were synthesized by our group and have shown high transfection efficiency and low cytotoxicity.

PAMAM-R is a noble gene delivery carrier due to its *in vivo* application, the wound healing of diabetic mice. It had good ability to deliver the gene

which can express growth factors into the cell of wound mouse-skin tissue. From inspiration of former successes like this, I attempted to apply PAMAM-R to in vivo experiment for dermal system and think this application is another appropriate approach for gene therapy. From the results, I knew which substructure in dermal tissue of hairless mouse PAMAM-R G4 can specifically deliver a target gene.

PAM-DET is also a well-developed carrier which accelerates the collapse membrane of endosom. But the unstable polyplex which is a complex of PAM-DET with a gene in aqueous solution with salt concentration could cause bad gene delivery efficiency. So, I tried to modify PAM-DET to sustain the stability of its polyplex for better transfaction effect. My main idea of the modification of PAM-DET was based on the conjugation of several moieties which are both hydrophobic and biocompatible on the primary amine of PAM-DET surface. The mechanisms of the conjugations were mainly the formation of amide or carbamate bond, and the linkage using of ring-opening reagent, Traut's reagent. In the final analysis of stability and the results from transfection of the polyplex, the modificated PAM-EDTs showed their enhanced stability at the state of the polyplex with a target gene in hydrophilic environment.

In the first part, I tried to conjugate the nontoxic and hydrophobic groups deoxycholate (DC), dimethyl-beta-cyclodextrin (DMβCD), and

dexamethasone (DX) with PAM-DET and synthesized PAM-DET-DC PAM-DET-DMβCD, and PAM-DET-DX. In comparison with PAM-DET, all hydrophobic group-conjugated PAM-DET dendrimers showed polyplexes (gene-polymer complexes) with better and longer size-stability in aqueous solutions with high ion strengths. The modified PAM-DET gene carriers showed higher transfection efficiency than PAM-DET and cytotoxicity levels equivalent to that shown by PAM-DET in HeLa and U87MG Cell lines.

In second part, I attempted to deliver a green fluorescent protein (GFP) gene into animal dermal tissue by using its polyplex with PAMAM-R, a gene-delivery carrier that has shown a high transfection efficiency and low cytotoxicity in our studies. Using green fluorescence images and a western blot assay, I showed the potential capability of PAMAM-R to act as a gene-delivery carrier to sub-organisms in the skin.

Keywords: Gene delivery system, polyplex, PAMAM dendrimer, PAMAM-R, PAM-DET, dermal.

Student number: 2004-20482

List of Publications

Journals

1. **Effect of deoxycholate conjugation on stability of pDNA/polyamidoamine-diethylentriamine (PAM-DET) polyplex against ionic strength** , Yunseong Jeong, Geun-Woo Jin, Eunjung Choi, Ji Hyuk Jung, Jong-Sang Park , *Int. J. Pharm.* , 420(2), pp.366-370 (2011)
2. **Ion pairs of risedronate for transdermal delivery and enhanced permeation rate on hairless mouse skin** , So Hee Nam,Ying Ji Xu, Hyemi Nam, Geun-woo Jin, Yunseong Jeong, Songhi An and Jong-Sang Park , *Int. J. Pharm.* , 419(1-2), pp.114-120 (2011)
3. **Spectrofluorimetric Determination of Alendronate by Conjugation with the Rhodamine B Sulfonyl Group** , Yunseong Jeong, Jihye Park, Geun-woo Jin, and Jong-Sang Park , *B. Kor. Chem. Soc.*, 32(5), pp.1777-1780 (2011)
4. **Spectrofluorimetric Determination of Bisphosphonates with a Fluorescent Chemosensor, Zinpyr-1 · 2Zn2+** , Yunseong Jeong, Geun-woo Jin, Seul Ki Kim, Juyoung Yoon, Jong-Sang Park , *B. Kor. Chem. Soc.*, 32(1), pp.37-38 (2011)
5. **The Natural Product NI-07, Is Effective Against Breast Cancer Cells While Showing No Cytotoxicity to Normal Cells** , Lauren S. Gollahon, Yunseong Jeong, Velvetlee Finckbone, Kyungwoo Lee, Jong-Sang Park , *The Open Breast Cancer Journal* , 3, pp.31-44 (2011)
6. **Spectrofluorimetric Determination of Bisphosphonates in Biological Sample**

with a Fluorescent Chemosensor, NadDPA-2Zn2+ , Yunseong Jeong, Soon Young Kim, Geun-woo Jin, Songhie An, Jae Han Lee, A-reum Jeong, Yeonsoon Chio,Jong-In Hong,Jong-Sang Park , *B. Kor. Chem. Soc.*, 31(9), pp.2561

7. **Preparation of Polymeric Microparticles by Horizontal Rotating** , Jae-ryang Joo, Min Ju Shon, Yunseong Jeong, and Jong-Sang Park , *B. Kor. Chem. Soc.*, 30(12), pp.3066-3068
8. **Evaluation of Generations 2, 3 and 4 Arginine Modified PAMAM Dendrimers for Gene Delivery**, Hye Yeong Nam, Hwa Jeong Hahn, Kihoon Nam, Woo-Hyung Choi, Yunseong Jeong, Dong-Eun Kim, Jong-Sang Park, *Int. J. Pharm.* 363, 199-205

List of Tables

Part A. Effect of Hydrophobic Group Conjugation on Stability of pDNA / Polyamidoamine-diethylentriamine (PAM-DET) Polyplex against Ionic Strength

Table 1. The synthetic parameters for PAM-DET-DC 23

Table 2. The synthetic parameters for PAM-DET-DMβCD 24

Table 3. The synthetic parameters for PAM-DET-DX 25

List of Figures

Part A. Effect of Hydrophobic Group Conjugation on Stability of pDNA / Polyamidoamine-diethylentriamine (PAM-DET) Polyplex against Ionic Strength

Figure 1. Three hydrophobic compounds for conjugation with PAM-DET 26

Figure 2a. Synthetic scheme for PAM-DET-DC 27

Figure 2b. Synthetic scheme for PAM-DET-DMβCD 28

Figure 2c. Synthetic scheme for PAM-DET-DX 29

Figure 3a. ^{1}H-NMR spectrum of PAM-DET and PAM-DET-DC 30

Figure 3b. ^{1}H-NMR spectrum of PAM-DET and PAM-DET-DMβCD 31

Figure 3c. ^{1}H-NMR spectrum of PAM-DET and PAM-DET-DX 32

Figure 4. Time-dependent profile of PAM-DET-DC polyplex 33

Figure 5. Time-dependent profile of PAM-DET-DMβCD polyplex 34

Figure 6. Time-dependent profile of PAM-DET-DX polyplex 35

Figure 7. Time-dependent profile of PAM-DET-DC(10) polyplex 36

Figure 8. Time-dependent profile of PAM-DET-DMβCD(8) polyplex 37

Figure 9. Time-dependent profile of PAM-DET-DX(10) polyplex 38

Figure 10. Transfection efficiency of PAM-DET-DC(10) 39

Figure 11. Transfection efficiency of PAM-DET-DMβCD(8) 40

Figure 12. Transfection efficiency of PAM-DET-DX(10) 41

Figure 13. Cell Viability test of PAM-DET-DC(10) 42

Figure 14. Cell Viability test of PAM-DET-DMβCD(8) 43

Figure 15. Cell Viability test of PAM-DET-DX(10) 44

Part B. Application of Polyamidoamine-Arginine(PAMAM-R) to Mouse Skin as a Method of Gene Delivery

Figure 1. The detail structures of hair follile of mamal's skin 58

Figure 2. Time-lapse fluorescence optical images 59

Figure 3. Time-lapse fluorescence optical images 60

Figure 4. Time-lapse fluorescence optical images 61

Figure 5. Time-lapse fluorescence optical images 62

Figure 6. Confocal images of HF of a 4-week-old hairless mouse 63

Figure 7. Confocal images of HF of a 5-week-old hairless mouse 64

Figure 8. Western bolt assay 65

Part A. Effect of Hydrophobic Group Conjugation on Stability of pDNA / Polyamidoamine-diethylentriamine (PAM-DET) Polyplex against Ionic Strength

1. Abstract

Polyplexes formed from cationic polymer/pDNA are known to be vulnerable to external ionic strength. To improve polyplex stability against ionic strength, I attempted to chemically conjugate 3 hydrophobic moieties, deoxycholate (DC), dimethyl-beta-cyclodextrin (DMβCD), and dexamethasone (DX), to the polyamidoamine–diethylenetriamine (PAM-DET) dendrimer. Dynamic light scattering studies showed that the resulting conjugated PAM-DETs had better tolerance than that of PAM-DET to ionic strength. In addition, I confirmed that polyplex stability is strongly related to the degree of conjugation of the DC, DMβCD, and DX moieties to the PAM-DET dendrimer and the charge ratio of each conjugated PAM-DET. Furthermore, the transfection efficiency of the PAM-DET-DC, PAM-

DET-DMβCD, and PAM-DET-DX polyplexes is generally higher than that of PAM-DET, although their cytotoxicities are the same. Therefore, chemical conjugation of these hydrophobic groups is a safe and effective method for increasing the stability of supramolecules formed from electrostatic interaction.

2. Introduction

Supramolecules, such as micelles, liposomes, and nanoparticles, have recently received much attention in the fields of fundamental, material, and applied sciences [1-3]. It has been reported that these supramolecules are formed via several attractive forces, including van der Waals forces, hydrophobic interactions, and electrostatic forces [4-7]. Among them, hydrophobic interactions have long been studied as the driving force for the formation of supramolecules. However, hydrophobic interactions have been recognized as unsuitable for the encapsulation of water-soluble biological substances, such as DNA, siRNA, and proteins, which have recently received attention for their high potential as therapeutic agents [9-11]. In contrast, electrostatic interactions have been suggested to be the most suitable driving forces for the encapsulation of biological substances to form nanoscale

supramolecules. However, the fragility of supramolecular structures formed by electrostatic forces, which is caused by increases in ionic strength, has been indicated as a weak point that must be overcome. Various methods for enhancing the stability of supramolecules formed by electrostatic interactions against ionic strength have been investigated for a wide range of applications [13-15]. One of the approaches involves the introduction of another attractive force, i.e., hydrophobic interactions by conjugation of a hydrophobic moiety, to increase the stability [1]. A polyamidoamine-diethylenetriamine (PAM-DET) dendrimer that was previously synthesized by our group [19] exhibits a highly positive charge on its surface and can form nanosized complexes with negatively charged pDNA through electrostatic interactions. Due to its high transfection efficiency and low cytotoxicity, PAM-DET has high potential as a gene-delivery carrier; however, it has low stability in environments with high ionic strength because its polyplex is formed via electrostatic interactions.

In this study, I attempt to increase the stability of the pDNA/PAM-DET complex against ionic strength by introducing 3 hydrophobic moieties, i.e., deoxycholate (DC), dimethyl-beta-cyclodexrine (DMβCD), and dexamethasone (DX) (Figure 1). DC is a well-known, non-toxic, natural fat emulsifier, and DMβCD is a widely studied, non-

toxic, bioavailable chemical as well as an absorption enhancer used in nasal drug administration [22-23]. The cytotoxicity and transfection efficiency of DX have already been confirmed by our group, and positive results in the development of other gene delivery carriers [24, 25] have shown that it is a suitable hydrophobic candidate. Therefore, conjugation of these groups could potentially enhance the stability of the complexes without causing undesirable increases in cytotoxicity. Through a dynamic light scattering (DLS) study, I show that conjugation of each group enhances the stability of the pDNA/PAM-DET complex. Furthermore, I compare the transfection efficiency and cytotoxicity of hydrophobic group–conjugated PAM-DET and non-conjugated PAM-DET to check for the possible negative effects of this conjugation on transfection efficiency and cytotoxicity. Interestingly, these conjugated PAM-DET polyplexes exhibit improved transfection efficiency while maintaining the low cytotoxicity of the PAM-DET polyplex. These results imply that conjugation of hydrophobic group is a simple and effective method for enhancing the stability of supramolecules formed by electrostatic interactions without introducing cytotoxicity.

3. Materials and methods

Materials

Polyamidoamine (PAMAM)-NH_2 G3, diethylenetriamine (DETA), DC, DMβCD, triethylamine (TEA), 1,1′-carbonyldiimidazolate (CDI), dimethylsulfoxide (DMSO), hexane, tetrahydrofuran (THF), *N*-hydroxybenzotriazole (HOBt), *N,N*′-dicyclohexylcarbodiimide (DCC), polyethyleneimine (PEI) 25-kDa, (3-[4, 5-dimethylthiazol-2-yl]-2, 5-diphenyltriazolium bromide (MTT), and NaCl were purchased from Sigma-Aldrich (St. Louis, MO). Dexamethasone (DX) mesylate was purchased from Steraloids Inc. (Newport, RI). Traut's reagent (C_3H_7NS·HCl) was obtained from Pierce (Iselin, NJ). A micro BCA™ protein assay kit (Pierce, Rockford, IL), luciferase 1000 assay system, and reporter lysis buffer (Promega, Madison, WI) were used for the transfection tests. For the transfection and cytotoxicity experiments, Dulbecco's modified Eagle's medium (DMEM), trypsin-ethylenediaminetetraacetic acid (EDTA), antibiotic, fetal bovine serum (FBS), and 1× phosphate-buffered saline (PBS) were purchased from GIBCO (Gaithersburg, MD). All chemicals were used without further purification. The firefly luciferase expression plasmid pCN-Luci was constructed by subcloning *Photinus* luciferase cDNA with the 21 amino acid nuclear localization signal from the Simian vacuolating virus 40

(SV40) large T antigen into pCN.

Synthesis of PAM-DET-DC

PAM-DET was synthesized as previously described [19]. To conjugate DC onto the surface of PAM-DET, amide bonds were formed using coupling reagents such as DCC and HOBt (Figure 2a). First, 50 mg of PAM-DET was dissolved in 50 mL of DMSO. Subsequently, DCC, HOBT, and DC were added at a constant equimolar ratio; the amount of DC was determined by the target degree of conjugation. Then, the reaction mixture was stirred at 50°C for 1 day. The reaction mixture was transferred in a dialysis bag and dialyzed in distilled water at 4°C. After 24 h, the purified solution was lyophilized to obtain highly viscous products. The resulting PAM-DET-DC product was analyzed by ^{1}H NMR at 40°C to calculate the actual degree of conjugation. Each PAM-DET-DC conjugate was named based on its actual degree of DC conjugation (Table 1).

Synthesis of PAM-DET-DMβCD

PAM-DET was synthesized as previously described [19]. The whole reaction mechanism for the conjugation of DMßCD onto the surface of PAM-DET is depicted in Figure 2b. First, the DMßCD activation step

proceeded via substitution of the hydroxyl groups, which are the end groups of DMßCD, with CDI to form an ester bond. Equivalent amounts of DMßCD and CDI were mixed in DMF for 2 h at room temperature with fast stirring. After the work-up of this mixture in cold hexane to remove the imidazolate rings, the hexane solution was dried to obtain activated DMßCD. Then, as the next step, 50 mg of PAM-DET was reacted with activated DMßCD and excess TEA in 50 mL of anhydrous DMSO for 24 h in the dark to form amide bonds, followed by removal of the imidazolate rings. Subsequently, PAM-DET-DMßCD was synthesized. After dialysis in cold water (4°C), pure PAM-DET-DMßCD was obtained. The product was then obtained after freeze-drying. The resulting PAM-DET-DMßCD product was analyzed by ^{1}H NMR at 40°C to calculate the actual degree of conjugation. Each PAM-DET-DMßCD conjugate was named based on its actual degree of DMßCD conjugation (Table 2).

Synthesis of PAM-DET-DX

PAM-DET was synthesized as previously described [19]. The conjugation reaction was performed as previously reported with some modification [26]. The overall synthesis scheme is displayed in Figure 2c. Briefly, dexamethasone coupling to PAM-DET was performed with 4 equivalents of Traut's reagent and 4 equivalents of dexamethasone

mesylate in anhydrous DMSO for 4 h at room temperature. An equal volume of water was added to the reaction mixture, and it was dialyzed against pure water and filtered through a 0.45-μm syringe filter to remove insoluble impurities. The product was then obtained after freeze-drying. The resulting PAM-DET-DX product was analyzed by ^{1}H NMR at 40°C to calculate the actual degree of conjugation. Each PAM-DET-DX conjugate was named based on its actual degree of DX conjugation (Table 3).

DLS study

The pDNA/PAM-DET and pDNA/PAM-DET-DC polyplexes were prepared in 10 mM HEPES buffer (pH 7.4) by incubation at 25°C for 30 min. To prepare each polyplex sample with PAM-DET and PAM-DET-DC (2), (4), and (10) (their charge ratio of cationic polymer/pDNA was commonly 16) as the first group, 1 mg/mL of pDNA was used. For the second group, pDNA/PAM-DET and pDNA/PAM-DET-DC (10) polyplexes with charges of 4, 8, and 16 were also prepared, taking into consideration the molecular weight and actual degree of conjugation, as shown in Table 1. After preparing the polyplexes of both groups, the NaCl concentration was adjusted to 50 mM by the addition of 1 M NaCl (20×) to the buffer solution. Changes

in the sizes of the polyplexes were measured using a Malvern Zeta sizer 3000HAs (Malvern Instrument Ltd., Worcestershire, UK) at 10 min intervals for 1 h. The first and second PAM-DET-DMßCD and PAM-DET-DX polyplex groups (shown in Table 2 and Table 3, respectively) with pDNA were prepared in the same way as the PAM-DET-DC polyplexes and were measured under the same conditions with same charge ratio as the PAM-DET-DC polyplex samples.

Cell culture

Human cervical cancer (HeLa) cells and human glioblastoma-astrocytoma cells (U87MG) were grown in DMEM containing 10% FBS and 1% antibiotic. Cells were incubated in plastic tissue culture cell binder flasks (Corning) at 37°C in a 5% CO_2 humidified incubator.

Transfection tests

To confirm the transfection efficiency of the PAM-DET and PAM-DET-DC polyplexes, transfection experiments were performed using HeLa and U87MG cells. Cells were seeded at 30,000 cells/well in 24-well plates in 600 μL of DMEM containing 10% FBS and 1% antibiotic and incubated at 37°C for 1 day. The cells were treated with a polyplex

solution prepared using 2 μg of pDNA and cationic polymer (PAM-DET, PAM-DET-DC (10), and PEI) at different charge ratios in 150 μL of FBS-free DMEM and incubated for 30 min at room temperature. After adding polyplex to each well, the cells were incubated for 2 days. For the assay, the growth medium was removed and the cells were washed with PBS and lysed with 150 μL of Reporter lysis buffer for 30 min at room temperature. The luciferase activity of the transfected cells was measured using an LB 9507 luminometer (Berthold, Germany) using 10 μL of lysate in the luminometer tube and automatic injection of 50 μL of luciferase assay reagent. All experiments were performed in triplicate. The transfection tests of PAM-DET-DMßCD (8) and PAM-DET-DX (10) were performed using the same procedure described above.

Cell viability

To measure the cell viability of the polyplexes, MTT assays were performed. HeLa and U87MG cells were seeded at 10,000 cells/well in 96-well plates in 120 μL of DMEM with 10% FBS and 1% antibiotic and incubated at 37°C for 1 day prior to the addition of the polyplexes. PAM-DET and PAM-DET-DC (10) polyplexes containing 0.2 μg of pDNA at the same charge ratio as that in the transfection experiment

were prepared in 24 μL of FBS-free DMEM by incubation at room temperature for 30 min. After adding the polyplexes, the cells were incubated for an additional 48 h. Then, the cells were washed with PBS followed by the addition of 26 μL of filtered MTT solution (2 mg/mL in PBS). After incubation at 37°C for 4 h, the medium was removed from the wells and 150 μL of DMSO was added to dissolve the formazan crystals. The absorbance at 570 nm was measured using a microplate reader (Molecular Device Co., Menlo Park, CA), and cell viability was calculated as a percentage relative to that of untreated control cells. The same procedure as described above was used for PAM-DET-DMßCD (8) and PAM-DET-DX (10).

4. Results and Discussion

Synthesis and characterization of PAM-DET-deoxycholate (PAM-DET-DC), PAM-DET-dimethy-beta-cyclodextrin (PAM-DET-DMβCD), and PAM-DET- dexamethasone (PAM-DET-DX)

To conjugate the DC moiety onto the surface of PAM-DET, an amide bond was formed between the carboxylic acid group of DC and the primary amine group of PAM-DET [17]. Synthesis of PAM-DET-DC, PAM-DET-DMßCD, and PAM-DET-DX was confirmed by ^{1}H NMR

spectroscopy (Figure 3a–3c). The signal at δ 2.48 was attributed to the protons of the secondary carbons (-*CH*$_2$*CH*$_2$-CH_2NH_2) in the interior of the PAM-DET molecule, as previously described [18, 19]. The group of signals between δ 0.72–2.23 (Figure 3a) was due to the protons of the multi-ring structure in deoxycholate [16]. The group of signals between δ 3.32–3.91 (Figure 3b) came from the protons of the multi-cyclodextrin rings in dimethy-beta-cyclodextrin [27]. The signals between δ 0.70–0.95 (Figure 3c) were attributed to the protons of the primary methyl groups in dexamethasone [28]. The ^{1}H NMR study showed successful conjugation of the DC moiety onto the PAM-DET surface. The average yield of DC, DMßCD, and DX conjugation was approximately 50% (Tables 1-3).

Dependence of polyplex stability against ionic strength on the degree of DC conjugation

It was reported that polyplex dissociation is accompanied by an increase in size to the micrometer level. Therefore, the stability of the polyplexes can be determined by observing changes in their size [2]. I determined the sizes of the polyplexes over time in an environment with increasing ionic strength (up to 50 mM) by the addition of concentrated NaCl solution. The size-increase profiles of the

polyplexes at 25°C were obtained by a DLS study. Different patterns were observed in the changes in sizes of the polyplexes formed from group A (PAM-DET; PAM-DET-DC (2), (4), and (10)), group B (PAM-DET; PAM-DET-DMßCD (1), (4), and (8)), and group C (PAM-DET; PAM-DET-DX (2), (5), and (10)). The polyplexes of pDNA/PAM-DET-DC (2), pDNA/PAM-DET-DMßCD (1), and pDNA/PAM-DET-DX (2) exhibited almost the same changes in size as PAM-DET, which implies that there is no contribution by any hydrophobic group to the stability of this polyplex due to the very low conjugation of the hydrophobic moiety. The polyplexes of pDNA/PAM-DET-DC (10), pDNA/PAM-DET-DMßCD (8), and pDNA/PAM-DET-DX (10) showed the slightest changes in size over 1 h compared with the other polyplexes in the groups (Figure 4-6). This result showed that the degree of conjugation of the hydrophobic moiety is an important factor for controlling the stability of the polyplex against ionic strength. Accordingly, a high degree of hydrophobic group conjugation onto PAM-DET leads to enhanced stability of the polyplex. A similar effect of hydrophobic moiety conjugation on cationic polymers was reported by other groups, thereby supporting our findings [1].

Dependence of polyplex stability against ionic strength on the charge ratio

It is well known that a sufficient amount of cationic polymer in relation to the amount of pDNA is required for the formation of a stable polyplex [20]. To explore the relationship between the charge ratio and the stability of polyplex in aqueous media with increased ionic strength, the stability of the polyplexes formed from PAM-DET and PAM-DET-DC (10) with various charge ratios were compared. As shown in Figure 7, the size of the PAM-DET polyplex at relatively low charge ratios (1:4 and 1:8) increased to almost 2 μm after 60 min. Upon the addition of NaCl, a slower increase in size was observed as the polyplexes formed with higher charge ratios from both PAM-DET and PAM-DET-DC (10). However, it seems that an increase in the charge ratio more effectively suppressed the growth of the polyplex formed from PAM-DET-DC (10) than that of the polyplex formed from PAM-DET. This result is probably due to in part to the increased amount of DC, as the charge ratio increased rather than it being solely an effect of the increased charge ratio. The PAM-DET-DMßCD (8) polyplexes in Figure 8 and the PAM-DET-DX (10) polyplexes in Figure 9 exhibited similar tendencies under the same charge ratio conditions.

Transfection efficiency and cytotoxicity

To determine the negative effects of conjugation of hydrophobic groups to PAM-DET, the transfection efficiency and cytotoxicity of conjugated PAM-DETs were tested. A transfection experiment comparing PAM-DET to PAM-DET-DC (10), PAM-DET-DMßCD (8), and PAM-DET-DX (10) in both HeLa and U87MG cells was performed. Interestingly, these conjugated PAM-DETs commonly showed higher transfection efficiency than PAM-DET in both cell lines (Figures 10-12). It was reported that increased transfection efficiency is caused by enhanced stability of the polyplex. Similarly, it seems that the enhanced stability of the polyplex due to conjugation of the hydrophobic moiety contributes to an increase in the transfection efficiency. The forte of DC and DMßCD as cell membrane penetration enhancers can also help insert the PAM-DET-DC and -DMßCD polyplexes into the cytosol and partially contribute to the positive transfection result, as suggested by Rojanasakul et al. [21] and Nicolaas et al. [22], respectively. Furthermore, all the conjugated PAM-DET polyplexes showed low cytotoxicity in both cell lines (Figure 13-15). In addition, dexamethasone, a potent glucocorticoid, also has positive properties. Dexamethasone can bind to glucocorticoid receptors after cellular entry, and the receptor/dexamethasone complex is subsequently translocated into the nucleus [29]. It suggests that the low cytotoxicity of PAM-

DET-DC, -DMßCD, and -DX is due to the biocompatibility of DC, DMßCD, and DX.

5. Conclusions

I successfully conjugated hydrophobic groups onto the surface of PAM-DET to produce PAM-DET-DC, PAM-DET-DMßCD, and PAM-DET-DX to form polyplexes with enhanced stability against ionic strength. We evaluated their stability by measuring the size of their polyplexes; each conjugated PAM-DET polyplex showed decreased growth compared to the PAM-DET polyplex in an environment with increased ionic strength, which implies that the conjugated PAM-DETs have enhanced stability against increased ionic strength. Furthermore, conjugation of hydrophobic groups caused a slight increase in the transfection efficiency without inducing toxicity. This strongly indicates that the introduction of hydrophobic moieties on PAM-DET is a good method to enhance polyplex stability against ionic strength without diminishing its advantageous properties, such as high transfection efficiency and low cytotoxicity.

6. References

1. Novel polyion complex micelles for liver-targeted delivery of diammonium glycyrrhizinate: in vitro and in vivo characterization.Yang, K.W., Li, X. W., Yang, Z. L., Ping, Z. L., Wang, F., Liu, Y., 2008. *J. Biomed. Mater. Res.* 88A, 140-148.

2. Novel Liposomal Formulation for Targeted Gene Delivery. Rivest, V., Phivilay, A., Julien, C., Belanger, S., Tremblay, C., Emond, V., Calon, F., 2007. *Pharm Res.* 24(5), 981-990.

3. Nano-sized octa-nuclear nickel cationic complex: Self-assembly on supramolecular level. Eremenko, I.L., Malkov, A.E., Sidorov, A.A., Fomina, I.G., Aleksandrov, G.G., Nefedov, S.E., Rusinov, G.L., Chupakhin, O.N., Novotortsev, V.M., Ikorskii, V.N., Moiseev, I.I., 2002. *Inorganica Chimica Acta.* 334, 334-342.

4. Formation of ordered arrays of gold nanoparticles from CTAB reverse micelles. Lin, J., Zhou, W., O'Connor, C.J., 2001. *Mater. Lett.* 49, 282-286.

5. Synthesis and agglomeration of gold nanoparticles in reverse micelles. Herrea, A. P, Resto, O., Briano, J. G., Rinaldi, C., 2005. *Nanotechnology.* 16, S618-S625.

6. Supercrystalline Colloidal Particles from Artificial Atoms. Zhuang, J., Wu, H., Yang, Y., Cao, Y.C., 2007. *J. Am. Chem. Soc.* 129, 14166-14167.

7. Dendrimers with Hydrophobic Cores and the Formation of Supramolecular Dendrimer-Surfactant Assemblies. Watkins, D.H., Sayed-Sweet, Y., Klimash, J.W., Torro, N.J., Tomalia, D.A., 1997.. *Langmuir.* 13, 3136-3141.

8. Supramolecular Architectures of Electrostatic Self-Assembled Glucose Oxidase Enzyme Electrodes. Calvo, E.J., Wolosiuk, A., 2004, *ChemPhysChem.* 5, 235-239.

9. Formation of Supramolecular Structures by Negatively Charged liposomes in the Presence of Nucleic Acids and Divalent Cations. Mozafari, M.R., Zareie, M.H., Piskin, E., Hasirci, V., 1998. *Drug Deliv.* 5, 135-141.

10. VEGF siRNA Delivery System Using Arginine-Grafted Bioreducible Poly(disulfide amine). Kim, S.H., Jeong, J.H., Kim, T., Kim, S.W., Bull, D.A., 2008. Mol. *Pharmaceutics.* 6, 718-726.

11. Switching by Pulse Electric Field of the Elevated Enzymatic Reaction in the Core of Polyion Complex Micelles. Atsushi, H., Kazunori, K., 2003. *J. Am. Chem. Soc.* 125, 15306-15307.

12. On-Off Control of Enzymatic Activity Synchronizing with Reversible Formation of Supramolecular Assembly from Enzyme and Charged Block Copolymers. Atsushi, H., Kazunori, K., 1999. *J. Am. Chem. Soc.* 121, 9241-9242.

13. Stabilized Nanocarriers for Plasmids Based Upon Cross-linked Poly(ethyleneimine). Neu, M., Sitterberg, J., Bakowsky, U., Kissel, T., 2006. *Biomacromolecules.* 7, 3428-3438.

14. Supramolecular Hydrophobic-Hydrophilic Nanopatterns at Electrified Interfaces. Klymchenko, A.S., Furukawa, S., Müllen, K., Auweraer, M.V., Feyter, S.D., 2007. *Nano Lett.* 7, 791-795.

15. Addition of "Charge-Shifting" Side Chains to Linear Poly(ethyleneimine) Enhances Cell Transfection Efficiency. Liu, X., Yang, J.W., Lynn, D.M., 2008. *Biomacromolecules.* 9, 2063-2071.

16. Proton magnetic resonance assay of total and taurine-conjugated bile acids in bile. Hiroki, I., Toshiaki, N., Koji, I., Hironori, M., Yoshiki, N., Yoshikuni, S., Takeshi, O., Kei, K., Yoshiteru, S., 1999. *J. Lipid Res.* 40, 1920-1924.

17. Enhanced transfection efficiency of PAMAM dendrimer by surface modification with L-arginine. Choi, J.S., Nam, K., Park, J., Kim, J.-B., Lee, J.-K., Park, J.-S., 2004. *J. Control. Release.* 99, 445-456.

18. Arginine-conjugated polypropylenimine dendrimer as a non-toxic and efficient gene delivery carrier. *Biomaterials.* Kim, T., Beak, J., Bai, C.Z., Park, J.-S., 2007. 28, 2061-2067.

19. PAMAM dendrimer with a 1,2-diaminoethane surface facilitates endosomal escape for enhanced pDNA delivery. Jin, G., Koo, H., Nam, K., Kim, H., Lee, S., Park, J.-S., 2011. *Polymer.* 52, 339-346.

20. PAMAM-PEG-PAMAM: Novel Triblock Copolymer as a Biocompatible and Efficient Gene Delivery Carrier. Kim, T., Seo, H.J., Choi, J.S., Jang, H.S., Beak, J., Kim, K., Park, J.-S., 2004. *Biomacromolecules.* 5, 2487-2492.

21. Mechanisms of action of some penetration enhancers in the cornea: Laser scanning confocal microscopic and electrophysiology studies. Rojanasakul, Y., Liaw, J., Robinson, J.R., 1990. *Int. J. Pharm.* 66, 131-142.

22. Nasal administration of an ACTH(4-9) peptide analogue with dimethyl-beta-cyclodextrin as an absorption enhancer: pharmacokinetics and dynamics. Nicolaas G.M. Schipper, 'J. Coos Verhoef, Larissa M. De Lannoy, Stefan G. Romeijn, Jan H. Brakkee, Victor M. Wiegant, Willem H. G., Frans W.H.M. M., 1993, *Br. J. Pharmacol.*, 110, 1335-1340.

23. Absorption of recombinant human granulocyte colony-stimulating

factor (rhG-CSF) and blood leukocyte dynamics following intranasal administration in rabbits. Watanabe Y., Matsumoto Y., Yamaguchi M., Kikuchi R., Takayama K., Nomura H., Maruyama K., Matsumoto M., 1993, *Biol Pharm Bull.,* 16(1):93-5.

24. Dexamethasone conjugated poly(amidoamine) dendrimer as a gene carrier for efficient nuclear translocation. Choi, J.S., Ko, K.S., Park, J.S., Kim, Y.-H., Kim, S.W., Lee, M., 2006. *Int. J. Pharm*., 320, 171-178

25**.** Dexamethasone-Conjugated Low Molecular Weight Polyethylenimine as a Nucleus-Targeting Lipopolymer Gene Carrier , Bae, Y.M., Choi, H., Lee, S., Kang, S.H., Kim, Y.T., Nam, K., Park, J.S., Lee, M., Choi, J.S., 2007. *BIOCONJ. CHEM*, 18, 2029-2036

26. Cationic corticosteroid for non-viral gene delivery. Gruneich, J.A., Price, A., Zhu, J., Diamond, S.L., 2004. *Gene Ther.* 11, 668–674.

27. A novel preparation of methyl-b-cyclodextrin from dimethyl carbonate and b-cyclodextrin. Gan Y, Zhang Y, Xiao C, Zhou C, and Zhao Y., 2011. *Carbohydr Res.* 346(3), 389-392.

28. Structure–transfection activity relationships with glucocorticoid–polyethylenimine conjugate nuclear gene delivery systems. Kun M., Minxin H., Yan Q., Liyan Q., Yi J., Jingmou Y, Bo L., 2009. *Biomaterials.,* 30, 3780–3789.

29. Cross-talk between pro-inflammatory transcription factors and glucocorticoids. Adcock IM., Caramori G., 2001. *Immunol Cell Biol.,* 79, 376–384.

Entry No.	Target degree of conjugation	Actual degree of conjugation	Name based on actual degree of conjugation	M_n
1	4	2	PAM-DET-DC(2)	17,318
2	8	4	PAM-DET-DC(4)	18,067
3	16	10	PAM-DET-DC(10)	20,314

Table 1. The synthetic parameters for PAM-DET-DC. Actual degree of conjugation and molecular weight of PAM-DET-DC were determined based on ^{1}H-NMR result.

Entry No.	Target degree of conjugation	Actual degree of conjugation	Name based on actual degree of conjugation	M_n
1	4	1	PAM-DET -DMβCD(1)	17,890
2	8	4	PAM-DET -DMβCD(4)	21,881
3	16	8	PAM-DET -DMβCD(8)	27,310

Table 2. The synthetic parameters for PAM-DET-DMβCD. Actual degree of conjugation and molecular weight of PAM-DET-DMβCD were determined based on ^{1}H-NMR result.

Entry No.	Target degree of conjugation	Actual degree of conjugation	Name based on actual degree of conjugation	M_n
1	4	2	PAM-DET-DX(2)	17,487
2	8	5	PAM-DET-DX(5)	18,865
3	16	10	PAM-DET-DX(10)	21,161

Table 3. The synthetic parameters for PAM-DET-DX. Actual degree of conjugation and molecular weight of PAM-DET-DX were determined based on ^{1}H-NMR result.

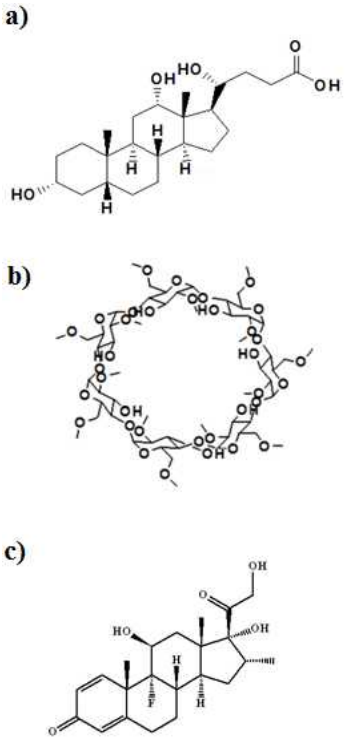

Figure 1. Three hydrophobic compounds for conjugation with PAM-DET. a) Deoxycholic acid (DC), b) Dimethyl-beta-cyclodexrine (DMβCD), c) dexamethasone (DX)

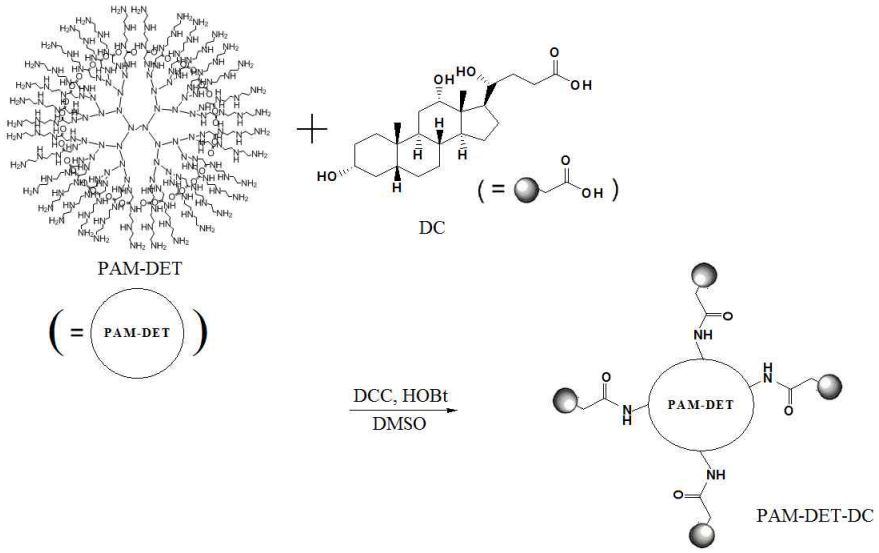

Figure 2a. Synthetic scheme for PAM-DET-DC

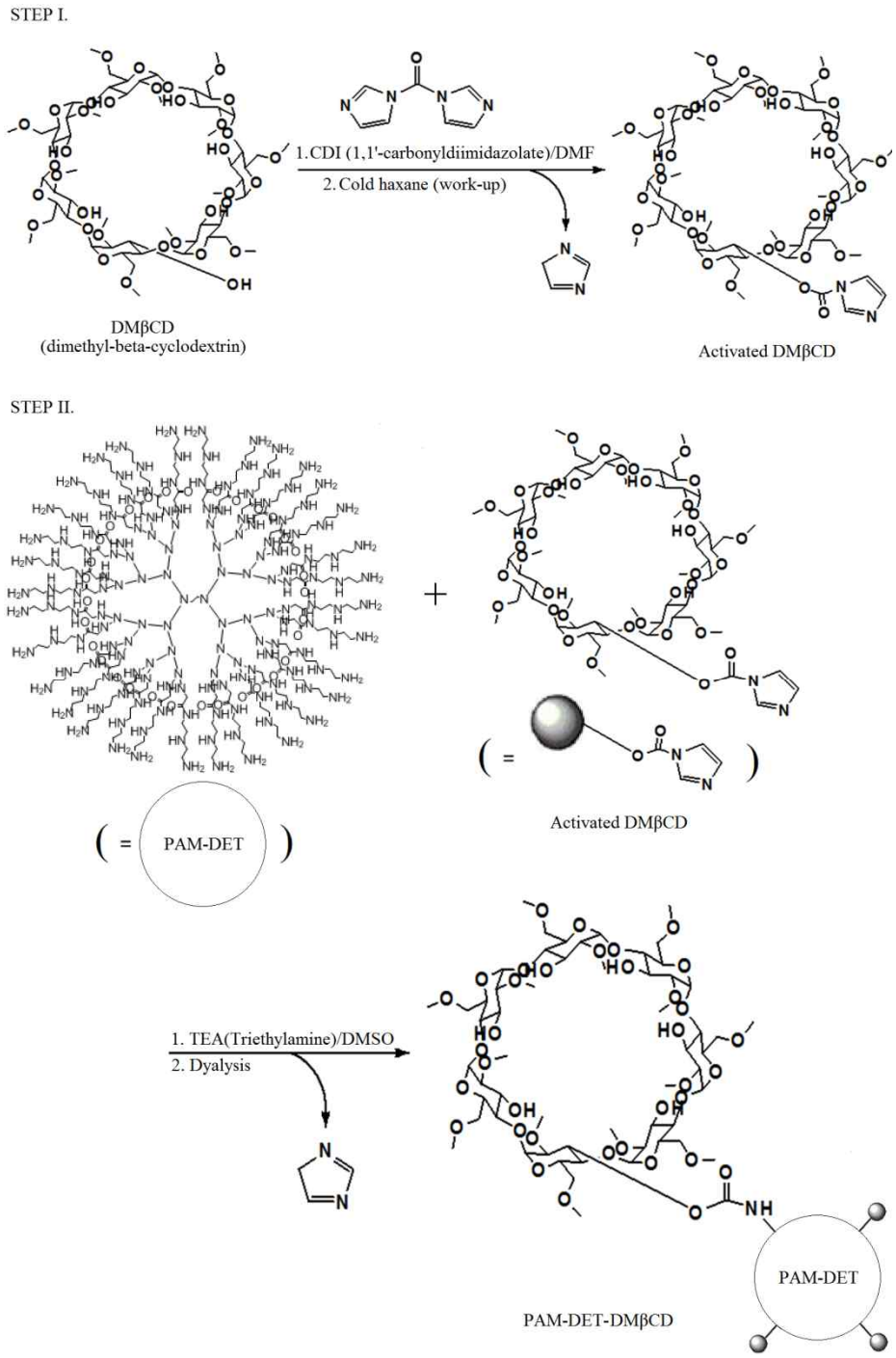

Figure 2b. Synthetic scheme for PAM-DET-DMβCD

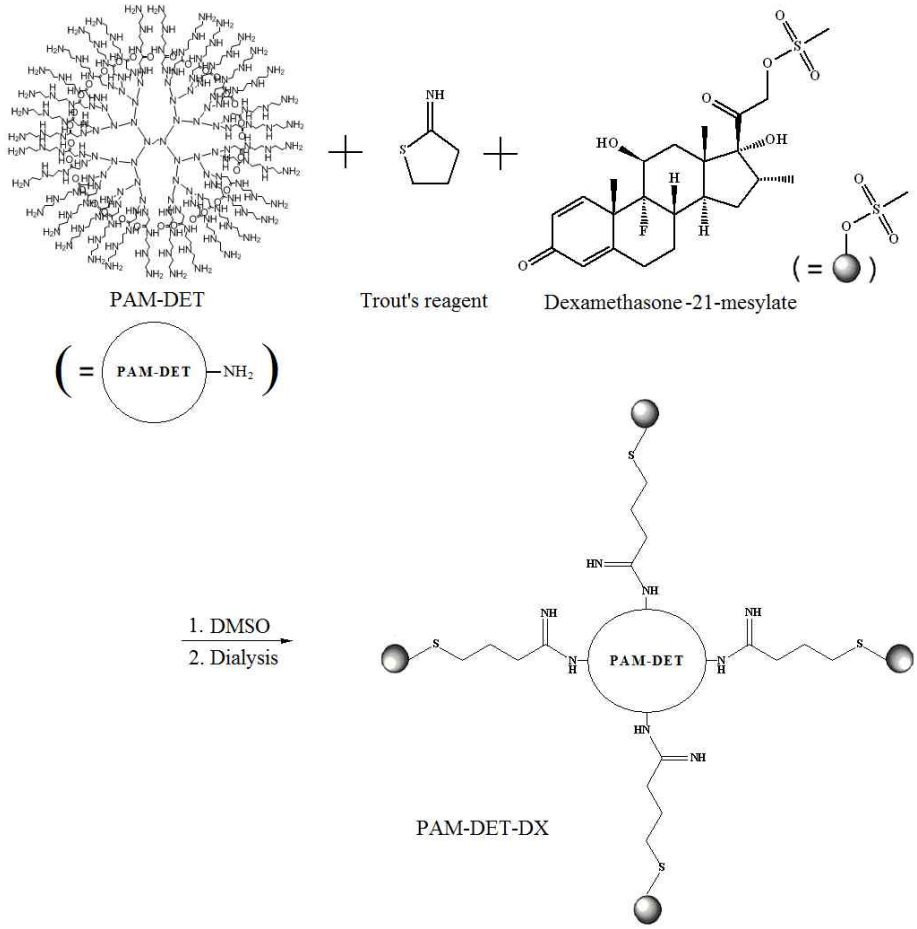

Figure 2c. Synthetic scheme for PAM-DET-DX

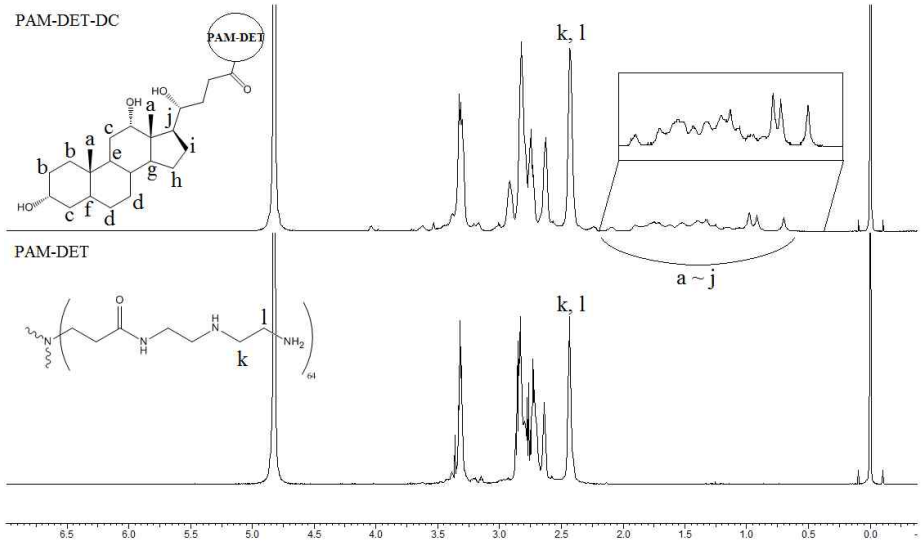

Figure 3a. ^{1}H-NMR spectrum of PAM-DET and PAM-DET-DC

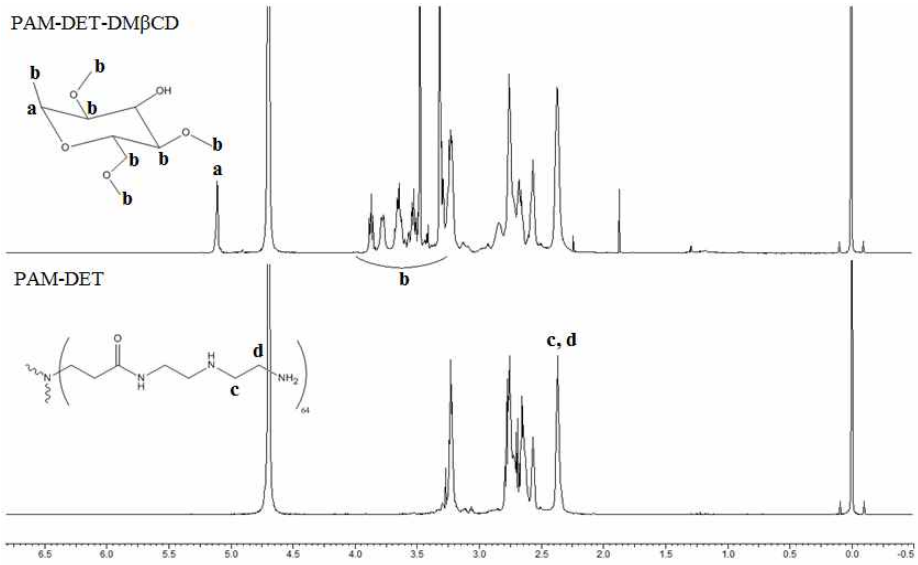

Figure 3b. ^{1}H-NMR spectrum of PAM-DET and PAM-DET-DMβCD

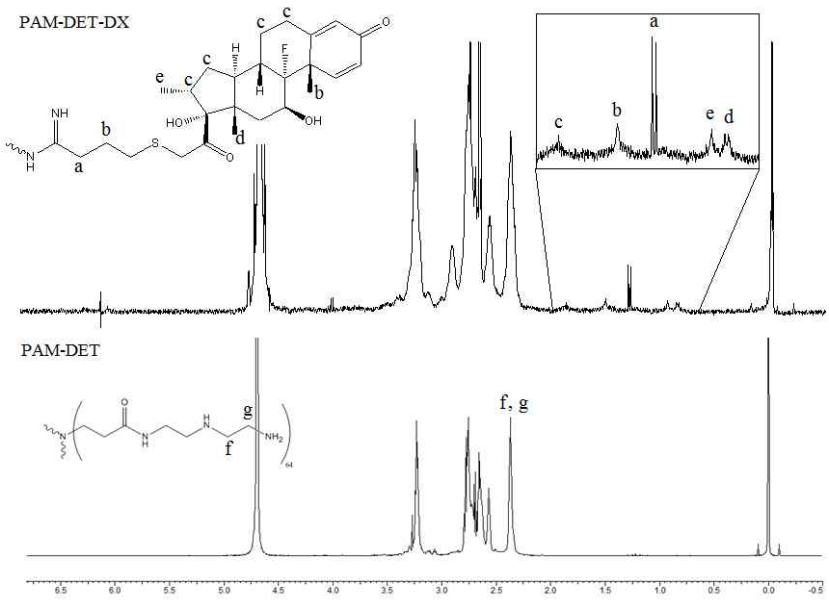

Figure 3c. ^{1}H-NMR spectrum of PAM-DET and PAM-DET-DX

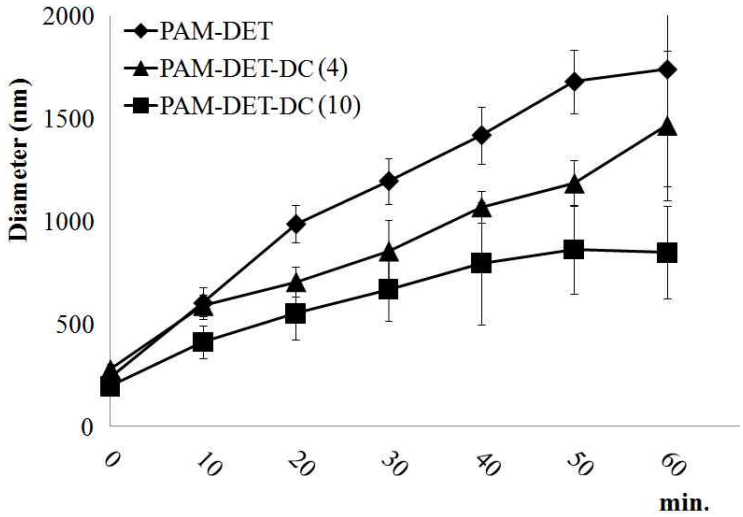

Figure 4. Time-dependent profile of PAM-DET-DC polyplex size under increased ionic strength (50 mM).

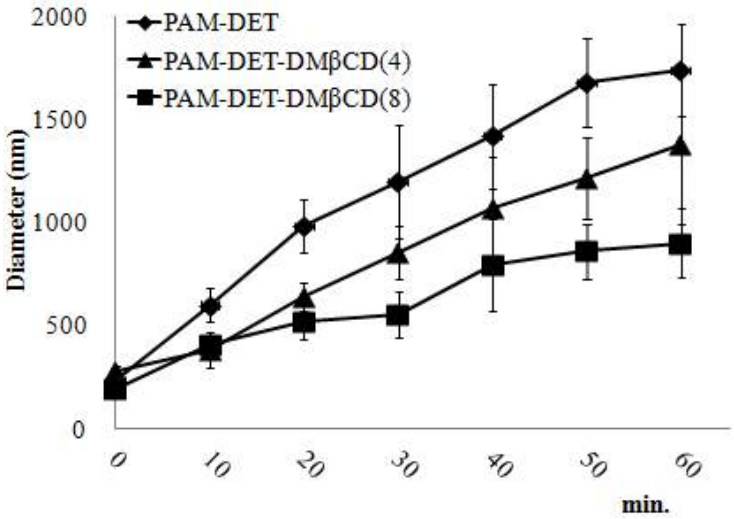

Figure 5. Time-dependent profile of PAM-DET-DMβCD polyplex size under increased ionic strength (50 mM).

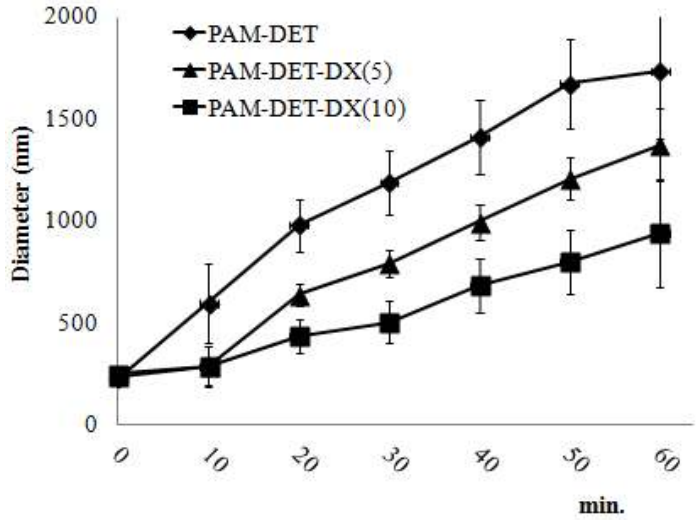

Figure 6. Time-dependent profile of PAM-DET-DX polyplex size under increased ionic strength (50 mM).

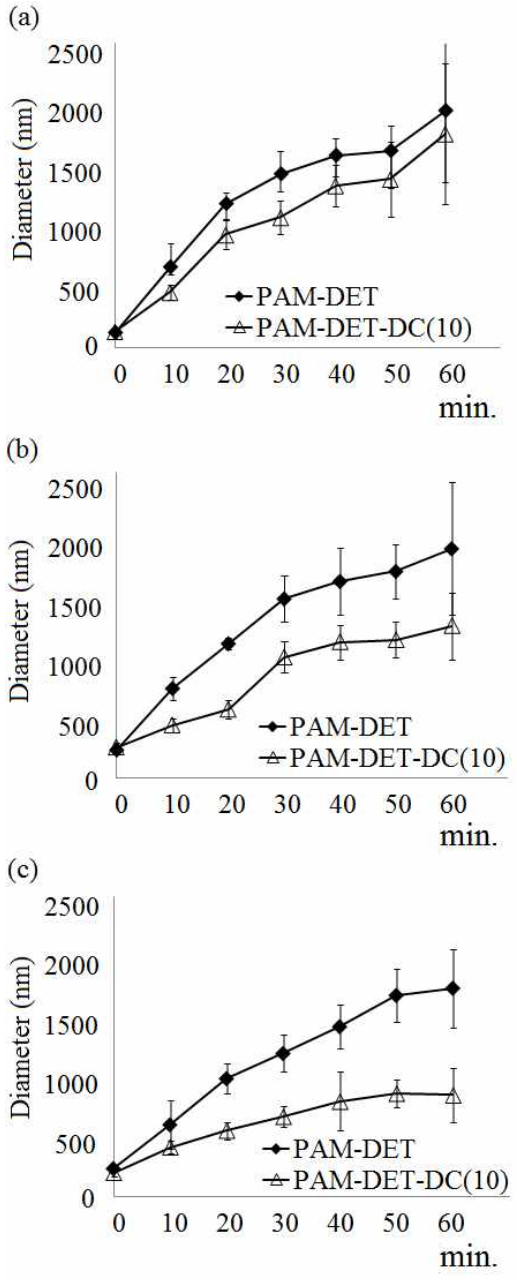

Figure 7. Time-dependent profile of PAM-DET-DC(10) polyplex size with varying charge ratio(+/- ; (a) 4, (b) 8, (c) 16) in 50 mM $NaCl_{(aq)}$.

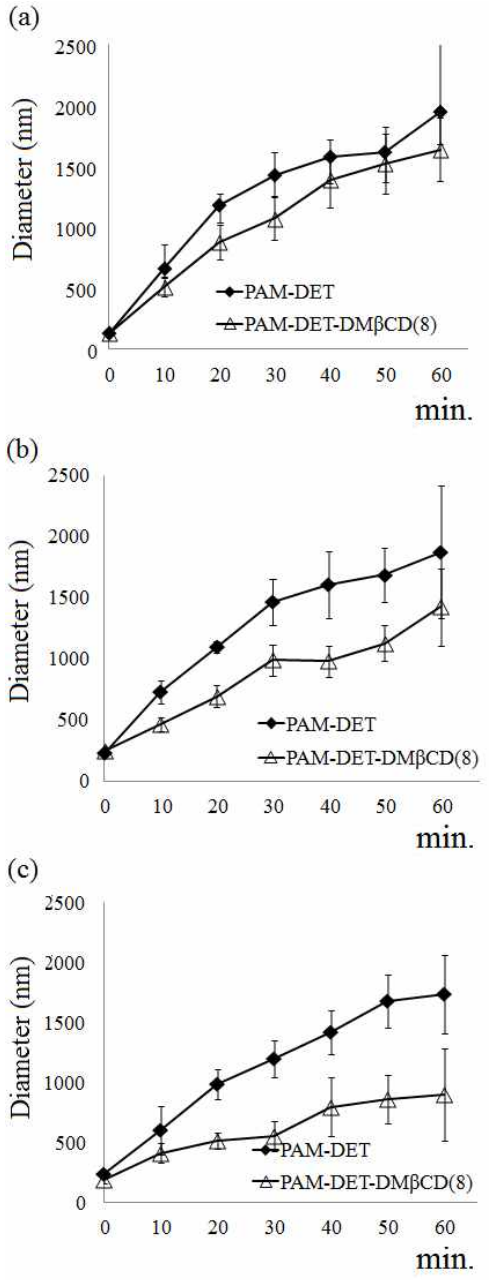

Figure 8. Time-dependent profile of PAM-DET-DMβCD(8) polyplex size with varying charge ratio(+/- ; (a) 4, (b) 8, (c) 16) in 50 mM $NaCl_{(aq)}$

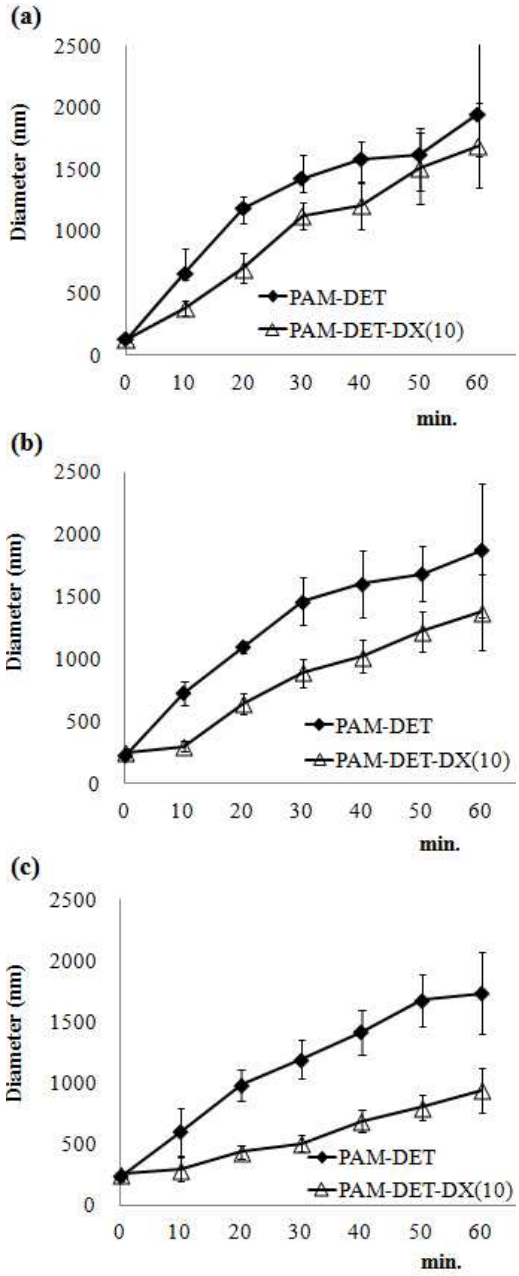

Figure 9. Time-dependent profile of PAM-DET-DX(10) polyplex size with varying charge ratio(+/- ; (a) 4, (b) 8, (c) 16) in 50 mM $NaCl_{(aq)}$

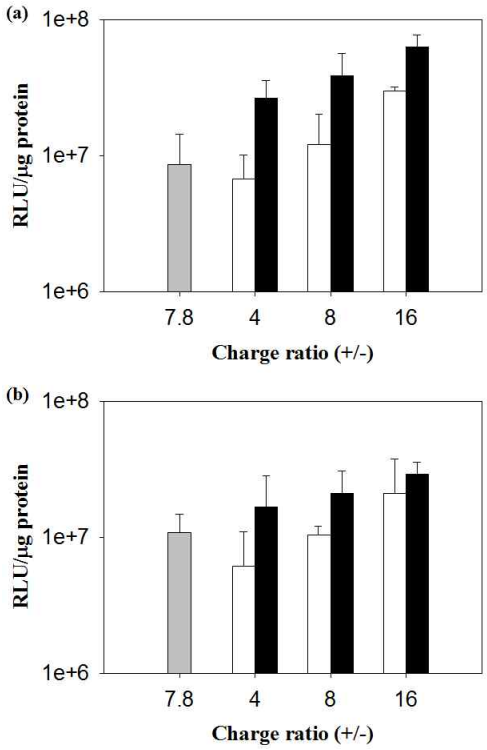

Figure 10. Transfection efficiency of PEI (gray bars), PAM-DET (white bars) and PAM-DET-DC(10) (black bars) against (a) HeLa and (b) U87MG cells.

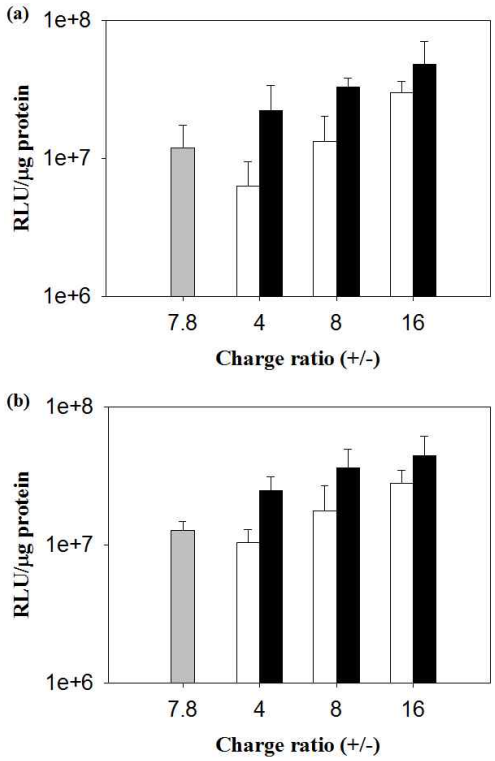

Figure 11. Transfection efficiency of PEI (gray bars), PAM-DET (white bars) and PAM-DET-DMβCD(8) (black bars) against (a) HeLa and (b) U87MG cells.

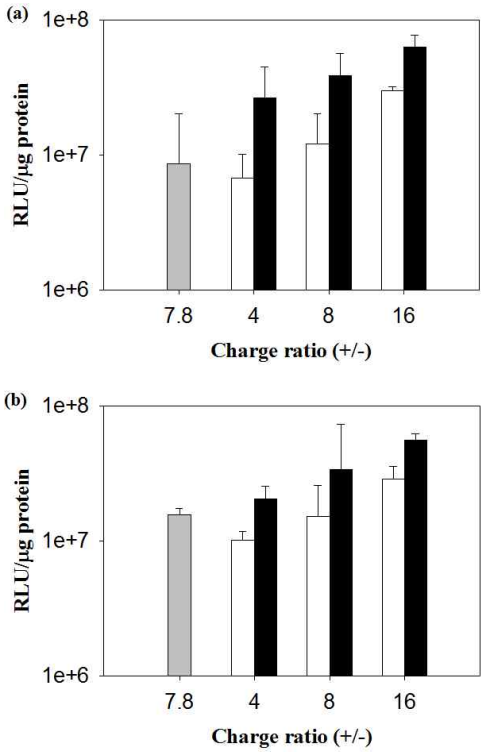

Figure 12. Transfection efficiency of PEI (gray bars), PAM-DET (white bars) and PAM-DET-DX(10) (black bars) against (a) HeLa and (b) U87MG cells.

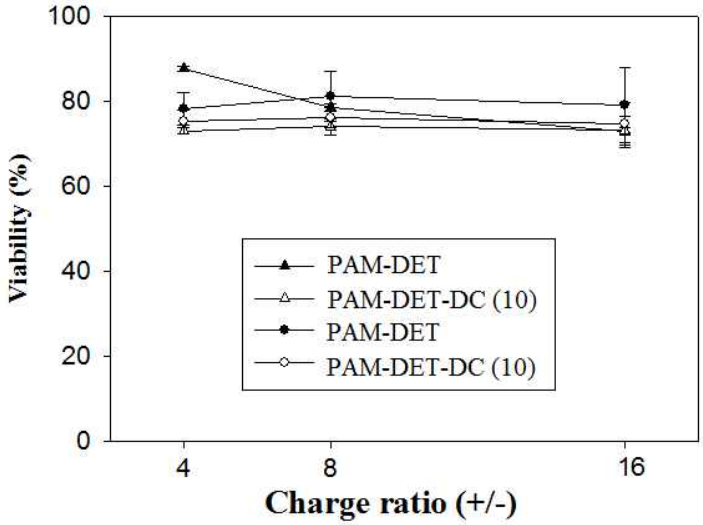

Figure 13. Cell Viability test of PAM-DET and PAM-DET-DC(10) polyplex varying charge ratio against HeLa (▲ and △) and U87MG cell (● and ○)

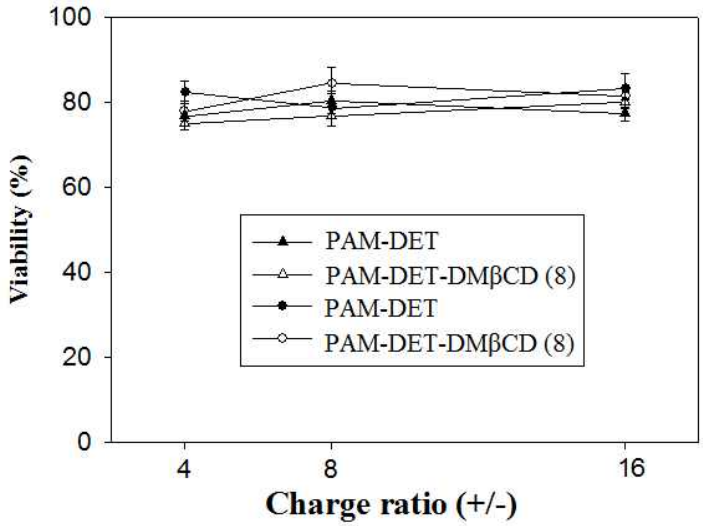

Figure 14. Cell Viability test of PAM-DET and PAM-DET-DMβCD(8) polyplex varying charge ratio against HeLa (▲ and △) and U87MG cell (● and ○)

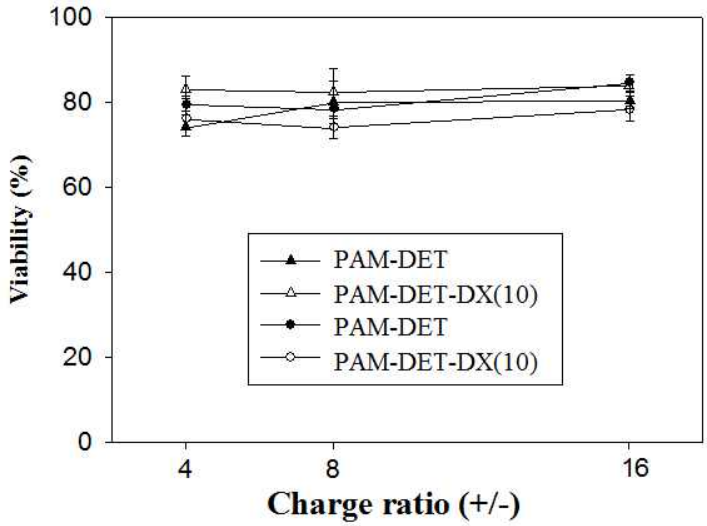

Figure 15. Cell Viability test of PAM-DET and PAM-DET-DX(10) polyplex varying charge ratio against HeLa (▲ and △) and U87MG cell (● and ○)

Part B. Application of Polyamidoamine-Arginine (PAMAM-R) to Mouse Skin as a Method of Gene Delivery

1. Abstract

The arginine-modified polyamidoamine (PAMAM) dendrimer—PAMAM-R G4—that was developed by our group in 2004 showed high transfection efficiency and low cytotoxicity in cell cultures and was therefore, a good carrier for gene delivery. In this study, I attempted to deliver a gene into mouse skin cells by direct dermal administration of PANAM-R (to form a polyplex). Subsequently, the plasmid DNA (pEGFP) was successfully delivered into the sub-organisms of skin tissue such as bulge, and the expression of green fluorescent proteins (GFPs) by these cells was confirmed by fluorescent optical and microscopic images and Western blot assay.

2. Introduction

A diverse range of nonviral gene delivery carriers, including cationic synthetic polymers, lipids, and peptides, have been developed and studied as alternatives to viral vectors owing to their merits, such as non-immunogenicity, high capacity for gene delivery, convenience of preparation and handling, and ease of introduction of therapeutic genes [1-3]. However, unexpected limitations have been encountered in gene therapy, such as low *in vivo* transfection efficiency and inherent cytotoxicity [4]. An arginine-modified dendrimeric polymer—PAMAM-R G4 (4th generation)—was developed by our group in 2007, and we confirmed that it has better transfection efficiency and lower cytotoxicity in cell-culture than PAMAM G4 [5]. We used plasmid DNA that coded for vascular endothelial growth factor (VEGF) and PAMAM-R G4 and developed a simple, non-viral method for gene therapy to improve wound healing on the skin of mice with diabetes and achieved interesting and desirable results in *in vivo* wound-healing tests [6].

In this study, I suggest another *in vivo* application of PAMAM-R G4. PAMAM-R G4 can be used as a dermal gene-delivery carrier for plasmid DNA coding for green fluorescent protein (pEGFP) in hairless

mice. Most of the biological agents, including genes, cannot be easily absorbed into mammalian skin because of the high degree of protection offered by skin tissue against external factors, such as air, water, and soil. However, researchers in the field of pharmaceutics and cosmetics have revealed that the hair follicle is one of the few sub-organisms of skin as a root that can facilitate transdermal absorption of some chemicals [7]. A hair follicle comprises many components [8] (Figure 1). Among them, the sebaceous gland, dermal papilla, and inner root sheath are in contact with the hair shaft, and these also have stem cells [9]. These stem cells are more active than normal cells; therefore, gene delivery into hair follicles and expression of the gene within its structure may be possible. Additionally, the hair follicle has already been introduced and studied as a notable target for gene therapy [8, 10, 15]. Alopecia, a condition characterized by hair loss, can be treated if a specific gene is effectively and stably delivered into the hair follicle.

Hence, I planned this study with the pEGFP/PAMAM-R G4 complex prior to the delivery of a target gene coding for the hair growth factor. I chose a hairless mouse model because the skin condition of this model was very similar to that of individuals with alopecia. I successfully delivered pEGFP with PAMAM-R G4 topically and observed GFP expression in the hair follicles of the mouse skin.

3. Materials and methods

Materials and instruments

PAMAM-R G4 was synthesized as previously described [5]. The target plasmid, pEGFP-C2, was purchased from BioLegend (San Diego, CA) and purified using a plasmid purification kit from Solgent (South Korea). Lipofectamine (Lipofectamine® 2000 Reagent) was purchased from Invitrogen (San Diego, CA), and polyethyleneimine (PEI) 25-kDa from was purchased from Sigma-Aldrich (St. Louis, MO). Fluorescent images were obtained using a fluorescence/optical camera, (Image Station 4000 MM, Eastman KODAK Company, Rocheter, NY, USA) and a green fluorescence image restoration microscope (DeltaVision RT; Applied Precision, Issaquah, WA). The anesthetic drugs used were Zoletil 50 (Virbac, Carros, France) and Rompun® 2% (Bayer, South Korea). An optical cutting temperature (OCT) frozen tissue fixer (OCT compound) was purchased from Tissue-Tek in Torrance, CA, USA. The primary (anti-GFP, anti-beta-actin) and the secondary (lgG) antibodies for western blotting were obtained from Millipore in Temecula, CA, USA. A Cryotome HM 505 E (MICROM, Germany), homogenizer (IKA® Work, China), and reporter lysis buffer (Promega, Madison, WI) were used during the treatment of skin tissue.

Preparation of mice

The model mice used in this study were male SKH1-hr (hairless) mice from Orient Bio., Ltd. (South Korea). Specifically, 4- or 5-week-old mice were used because their hair follicle cycle needed to reach anagen phase when cells in the hair follicle are more active than in the other phases [11]. But, 5- and 6-week-old mice were tested for comparison between anagen and catagen phase in the experiment of optical and fluorescence image. The mice were feed only water for 24 h before the experiments and cared for seriously, so as not cause them to be scared or rub their skin against others by single mouse caging. Mice were anesthetized with a 0.15 mL injection of Zoletil/Rompun mixture (3:1, v/v).

Methods of pEGFP loading and GFP expression

The pEGFP/PAMAM-R polyplex, pEGFP/PEI polyplex, and pEGFP/Lipofectamine lipoplex were prepared in distilled water at a gene/polymer mixing ratio of 1:4. The gene concentrations were commonly 1 mg/10 mL. Thirty minutes after the preparation of the polyplex and lipoplex solutions, they were administered onto the skin of an anesthetized mouse. The fluorescence images of the spot on the skin where the gene was loaded were observed after 1 day, 2 days, 4 days, and 7 days using the Image station.

The skin spot was then separated from mouse's body as a skin sample, and stored in a 10% sucrose aqueous solution for 4 h. Then, the skin sample was frozen and fixed flatways to form an OCT block in liquid OCT compound at -20°C. The block containing the skin sample was cross-sectioned into 10 μm thick slices with a Cryotome. Green fluorescence microscopy images were obtained of each skin sample slice. A control sample containing a non-gene loaded spot was also treated using the same procedure.

To lyse the cells and extract the GFP from the skin samples, 1–2 mg of the control and test (gene-loaded) skin tissue samples were finely ground in 2 mL of 5% reporter lysis buffer (Promega, Madison, WI) using a homogenizer for 24 h at 25°C. The supernatant (0.3 mL) was obtained from each sample after centrifugation for 10 minutes at 2500 (×*g*), then, a western blot of each supernatant solution was performed as previously described [12, 13] using proper antibodies; AB3080 (Anti-GFP, rabbit host), 04-1116(Anti-beta-actin, rabbit host) and 12-348 (The second antibody, Goat anti-rabbit lgG). Western blot probing was processed by enhanced chemical luminescence (ECL) solution (Amersham™, GE Healthcare, UK).

4. Results and Discussion

Optical images for green fluorescence

The fluorescent signals of the spots where the pEGFP/PAMAM-R polyplex, the pEGFP/PEI polyplex, and the pEGFP/Lipofectamine lipoplex were topically loaded were observed using a fluorescence camera and an Image Station (Figures 2 - 5). At the cases of 5-week-old mice (Figure 3, 4), they displayed the clear and sharp distinction of green signal between gene loaded area (highlighted spots) and not loaded are as the surround of the spots. The spot where the PAMAM-R G4 polyplex was loaded maintained its green fluorescent intensity for 2–4 days, compared to PEI polyplex and Lipofectamine polyplex spots, which showed no fluorescence signal from day 1 to day 7. At 7 days observation, the timid signals on the gene-unloaded area were caused as noise due to wrinkles which occurred from fixing the anesthetized mice on the plate of Image station that was operated in similar way of a picture scanner. The rest area of the dermis and epidermis, except for the hair follicle, is generally enough strong to protect against almost any chemical; therefore, I believed that the polyplexes and the lipoplex could be absorbed into the skin through the hair follicles. This result demonstrated that PAMAM-R G4 caused the target gene, pEGFP, to be

more easily absorbed and more efficiently delivered than PEI and Lipofectamine.

However, at the cases of 6-week-old mice, all of the fluorescent signals from PAMAM-R polyplex-loaded spot were too weaken to be detected on even the first day (Figure 4, 5). These results demonstrate that after the catagen phase (6th week after birth) in hair follicular cycle of mouse, is not easy and appropriate to deliver a gene into hair follicle because epidermis at catagen is dry and tough to tighten the ingress of hair follicle in order to sustain a grown hair shaft. Otherwise, epidermis at anagen phase (4th – 5th week after birth) is moist and soft to widen the ingress of hair follicle in order to help ease hair-growing out [16].

Hence, a mouse in anagen phase (4 or 5-week-old) is a more appropriate model than one in catagen (6 or 7-week-old) or telegen (8 – 12-week-old) phase to deliver a gene into hair follicle successfully.

Cross-sectioned images by fluorescence microscopy and western bolt assay for expressed GFP

To confirm that the GFP was really expressed in the hair follicles but not in other region or structures of the dermis or epidermis, I cross-sectioned the mouse skin samples and observed the fluorescence microscopy images (Figures 6 and 7). I specifically selected anagen mice (4 and 5-week-old mice) based on the result from the previous

experiment, the detection of optical images for green fluorescence.

In the every image, sebaceous gland and inner root sheeth couldn't be distinguishable but bulge in the hair follicle because a hairless mouse unlike normal mouse doesn't have hair shafts and their dermal papilla. The green fluorescent signals were clearly observed in the hair follicles and came from the hair follicles of both the test (treated with pEGFP/PAMAM-R polyplex) and control (not treated with pEGFP/PAMAM-R polyplex) sample, but their intensity values were very different; the value from the control samples was 105–125, while that of the test samples was 295–315. In addition, the western blot results confirmed that GFP was expressed only in the hair follicles of the test samples, and not in the control samples (Figure 8). Although mouse hair follicles have a basic green autofluorescence signal, both the fluorescence microscopy imaging and protein assay results show that topical administration of pEGFP/PAMAM-R polyplex can successfully deliver the target gene, pEGFP, and result in expression of the encoded protein, GFP in the hair follicles.

If the same method was applied to normal mouse skin, similar results may be not obtained because the absorption efficiency of the gene/polymer polyplexes would be lower than that in a hairless mouse without hair shafts due to hair shafts in normal mouse skin that block the entrance of the hair follicle.

5. Conclusions

I successfully delivered pEGFP to the hair follicles of hairless mouse skin using a gene delivery carrier, PAMAM-R G4. PAMAM-R G4,which was shown via the previous *in vitro* studies in cell-culture, [5, 14], is more effective for topical expression of a target protein than other non-viral carriers such as PEI and Lipofectamine in this study. An future trial using genes encoding various hair growth factors (IGFs) on mammalian skin will be expected as a novel treatment for the symptoms of hair thinning or hair loss, such as alopecia, atrichia, and baldness.

6. References

1. Kay MA, Liu D, Hoogerbrugge PM. *Gene therapy. PNAS,* 1997. 94: 12744-6.

2. Synthetic DNA delivery systems. Luo D and Saltman WM., 2000. *Nat Biotech.,* 18, 33-7

3. From simple transfection agents to artificial viruses. Mastrobattista E.,Bravo S.A., van der Aa M., Crommelin D.J.A., 2005. *Technologies.,* 2, 103-9.

4. β-Galactose staining following intracoronary infusion of cationic liposomes in the in vivo rabbit heart is produced by microinfarction rather than effective gene transfer: a cautionary tale. Wright M. J., Rosenthal E., Stewart L., Wightman L. M. L, Miller A. D., Latchman D. S.. 1998. *Gene Therapy.,* 5, 301.

5. Enhanced transfection efficiency of PAMAM dendrimer by surface modification with l-arginine. Choi J. S., Nam K., Park J., Kim J.-B., Lee J.-K., Park J.-S., 2004. *J CONTROL RELEASE*, 99(3), 445-456.

6. Effective healing of diabetic skin wounds by using nonviral gene therapy based on minicircle vascular endothelial growth factor DNA and a cationic dendrimer. Kwon MJ, An S, Choi S, Nam K, Jung HS, Yoon CS, Ko JH, Jun HJ, Kim TK, Jung SJ, Park JH, Lee Y, Park JS,

2012. *J Gene Med.* 14(4), 272-278.

7. Transdermal and topical drug delivery from theory to clinical practice. Adrian W..2003, *Pharmaceutical press,* 1-36.

8. The hair follicle as a gene therapy target. Robert M. H.. 2000. *Nat Biotechnol.,* 18, 23-21.

9. Capturing and profiling adult hair follicle stem cells.Morris R. J., Liu Y, Marles L, Yang Z, Trempus C, Li S, Lin J. S., Sawicki J. A., Cotsarelis G.. 2004. *Nat Biotechnol.,* 22, 411-7.

10. Gene delivery to the hair follicle. Ohyama M., Vogel J. C.. 2003. *J Investig Dermatol Symp Proc.*, 8, 204-6.

11. A Comprehensive Guide for the Accurate Classification of Murine Hair Follicles in Distinct Hair Cycle Stages. Sven M.-R., Bori H., Carina van der V., Stefan E., Kerstin F., Ian A M., Kurt S S., Ralf P.. 2001. *J Invest Derm.*. 117, 3–15.

12. Vector systems for heterologous expression of proteins in Saccharomyces cerevisiae. Martin F., Rainer N., Dominik M., Kayb B., Volker R., Thomas H., 2002. *Methods in Enzymology.,* 350, 248–257.

13. Mammalian formin-1 participates in adherens junctions and polymerization of linear actin cables. Agnieszka K., H. Amalia P., Elaine F.. 2003. *Nat Cell Biology*. 6, 21 – 30.

14. Enhanced transfection of primary cortical cultures using arginine-grafted PAMAM dendrimer, PAMAM-Arg**.** Kim J. B., Choi J. S., Nam K., Lee M., Park J.-S., Lee J.-K.. *J CONTROL RELEASE*., 114, 110–117

15. WNT Signaling in the Control of Hair Growth and Structure. Sarah E. M., Karl W., Patricia C. S., Henk R., Roel N., Daniel J. S., Gregory S. B.. 1999. *Developmental Biology.,* 207, 133–149

16. Controls of hair follicle cycling. K. S. Stenn and R. Paus. 2001. *Physiol Rev.,* 81, 449–494

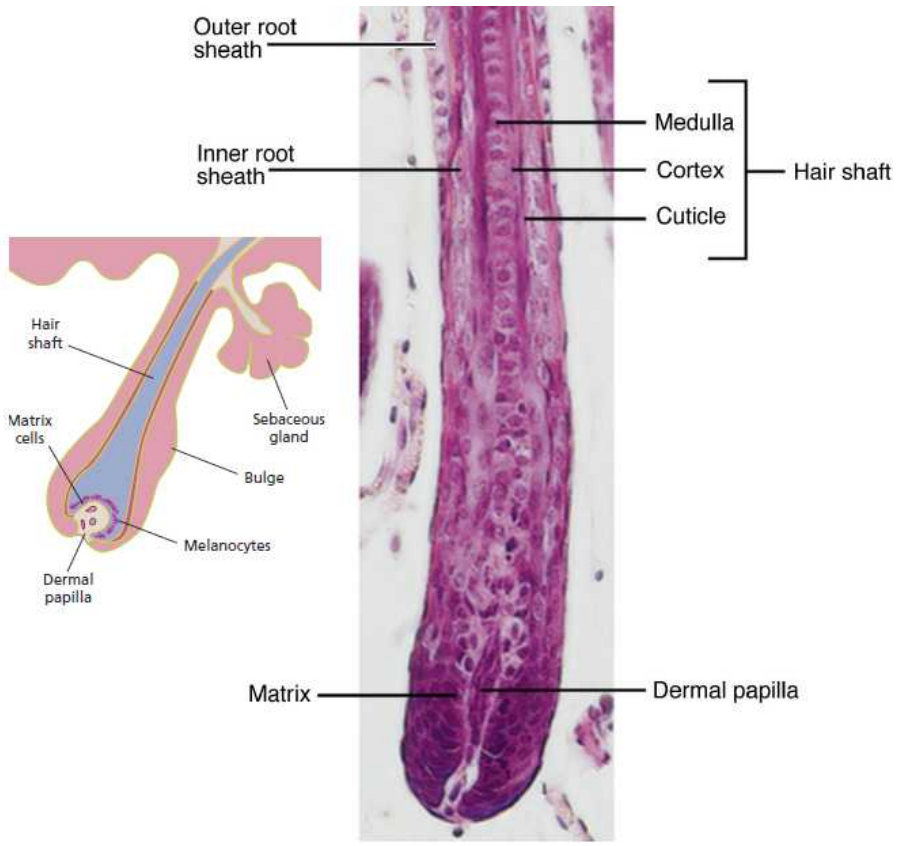

Figure 1. The detail structures of hair follile of mamal's skin. On the left is a illerstrated image of skin [8] , on the right is a horizontal cross-section of a hair follicle [15].

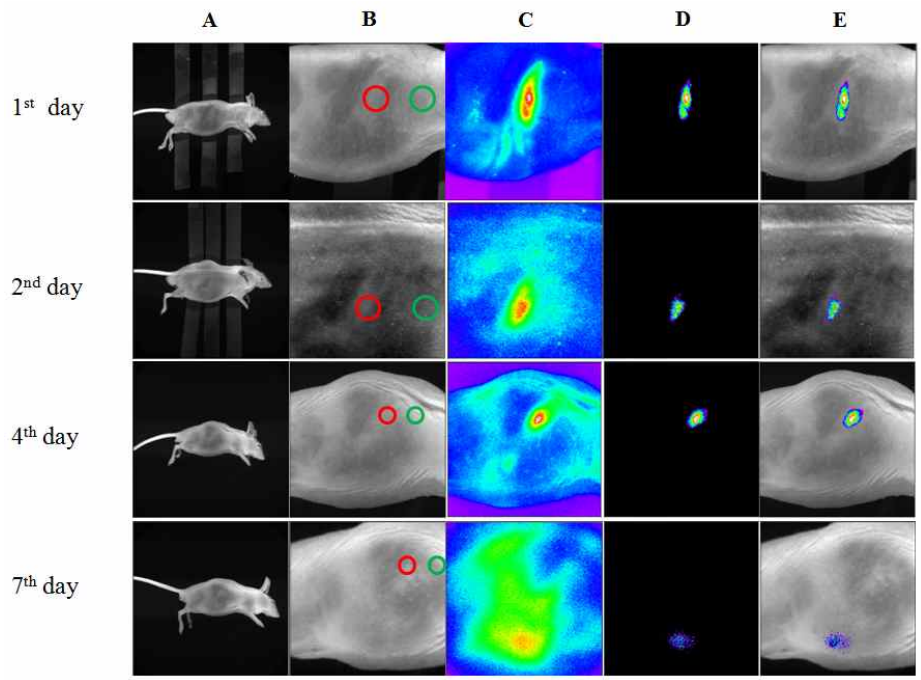

Figure 2. Time-lapse fluorescence optical images of a pEGFP/PAMAM-R G4 polyplex-loaded spot (red circles) and a pEGFP/PEI polyplex-loaded spot (green circles) on the skin of a 5-week-old hairless mouse. A-optical full size cut, B-optical zoomed cut, C-initial pictured fluorescence signal, D-adjusted fluorescence image of C, E-the merged image of B and D.

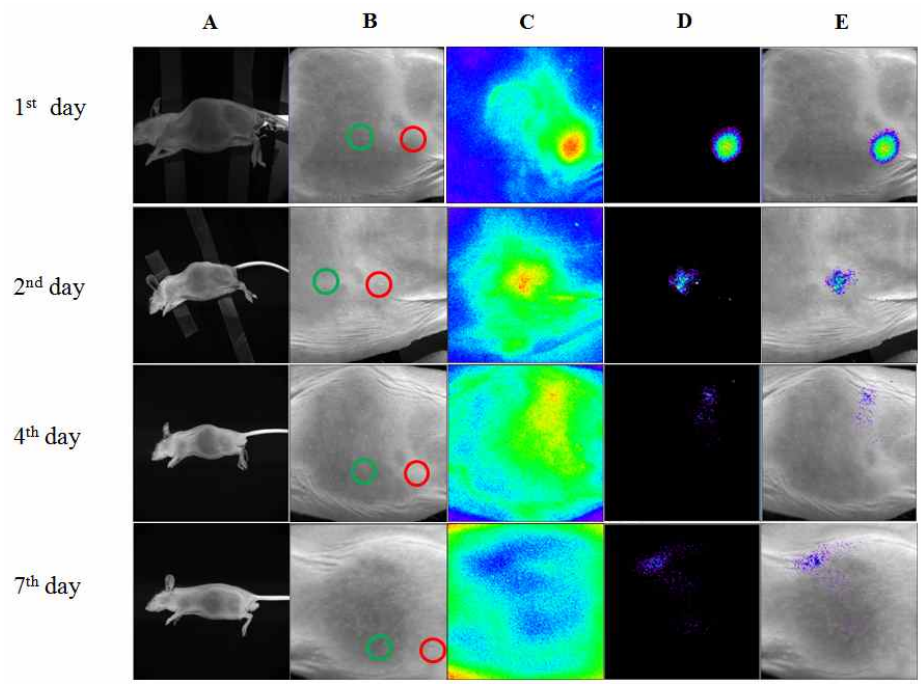

Figure 3. Time-lapse fluorescence optical images of a pEGFP/PAMAM-R G4 polyplex-loaded spot (red circles) and a pEGFP/PEI polyplex-loaded spot (green circles) on the skin of a 5-week-old hairless mouse. A-optical full size cut, B-optical zoomed cut, C-initial pictured fluorescence signal, D-adjusted fluorescence image of C, E-the merged image of B and D.

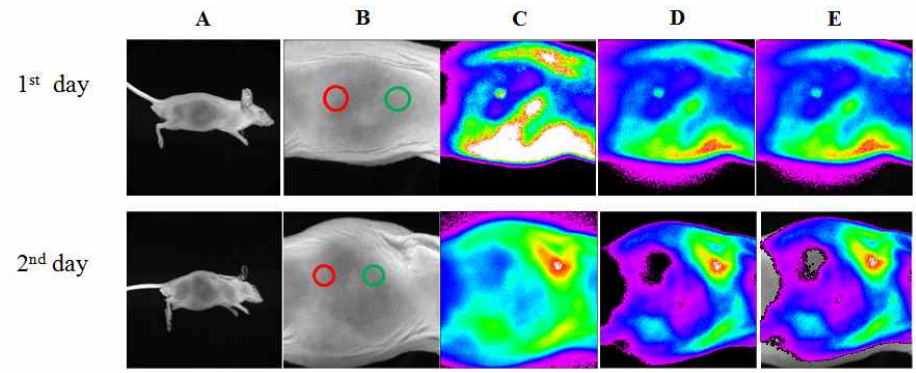

Figure 4. Time-lapse fluorescence optical images of a pEGFP/PAMAM-R G4 polyplex-loaded spot (red circles) and a pEGFP/PEI polyplex-loaded spot (green circles) on the skin of a 6-week-old hairless mouse. A-optical full size cut, B-optical zoomed cut, C-initial pictured fluorescence signal, D-adjusted fluorescence image of C, E-the merged image of B and D.

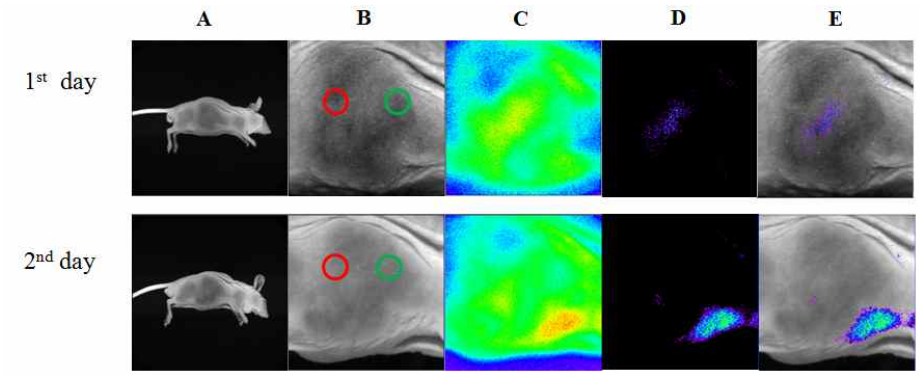

Figure 5. Time-lapse fluorescence optical images of a pEGFP/PAMAM-R G4 polyplex-loaded spot (red circles) and a pEGFP/PEI polyplex-loaded spot (green circles) on the skin of a 6-week-old hairless mouse. A-optical full size cut, B-optical zoomed cut, C-initial pictured fluorescence signal, D-adjusted fluorescence image of C, E-the merged image of B and D.

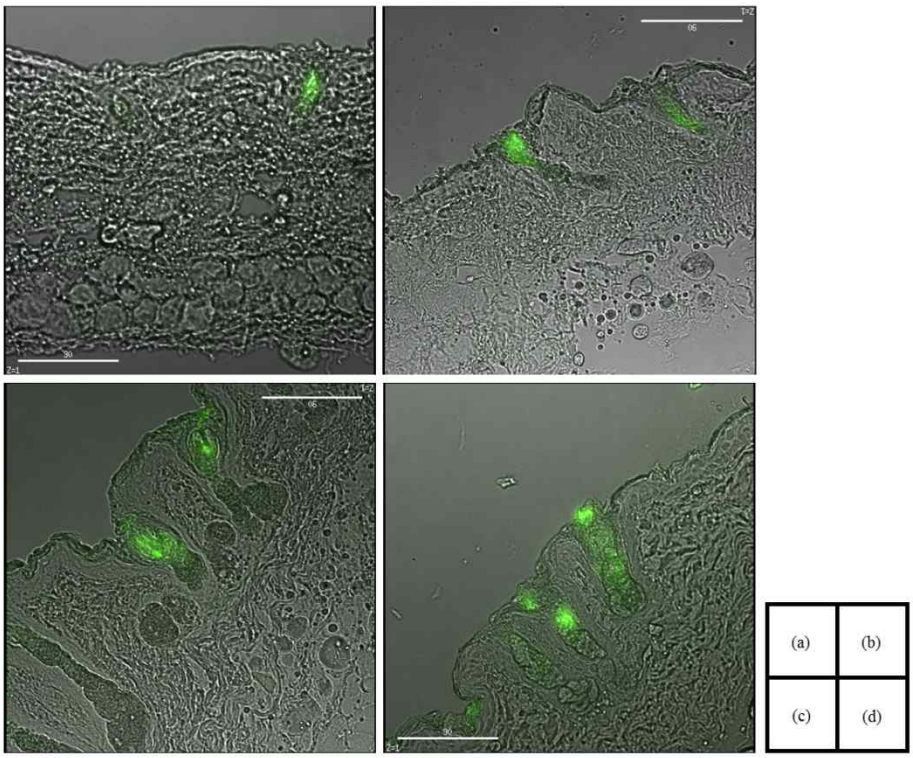

Figure 6. Fluorescence microscopy images of the hair follicles of a 4-week-old hairless mouse. (a) and (b) are from the control samples on which the EGFP gene was not loaded, (c) and (d) are from the test samples on which the EGFP gene was pEGFP/PAMAM-R G4 polyplex-loaded. Scale bars in each image read 90 μm.

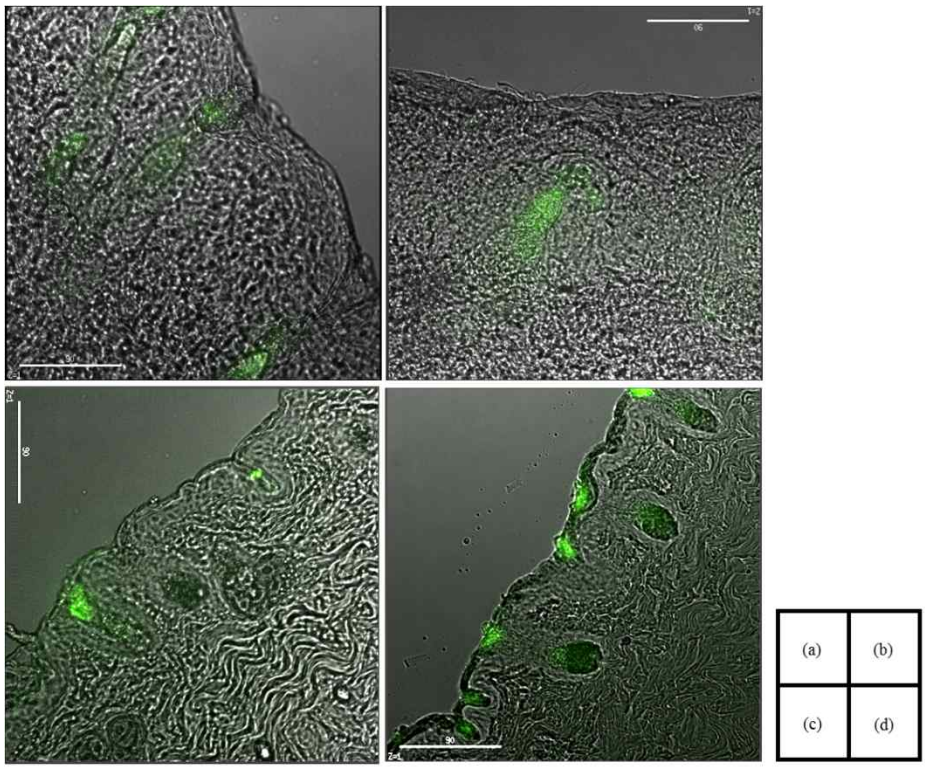

Figure 7. Fluorescence microscopy images of the hair follicles of a 5-week-old hairless mouse. (a) and (b) are from the control samples on which the EGFP gene was not loaded, (c) and (d) are from the test samples on which the EGFP gene was loaded. Scale bars in each image read 90 μm.

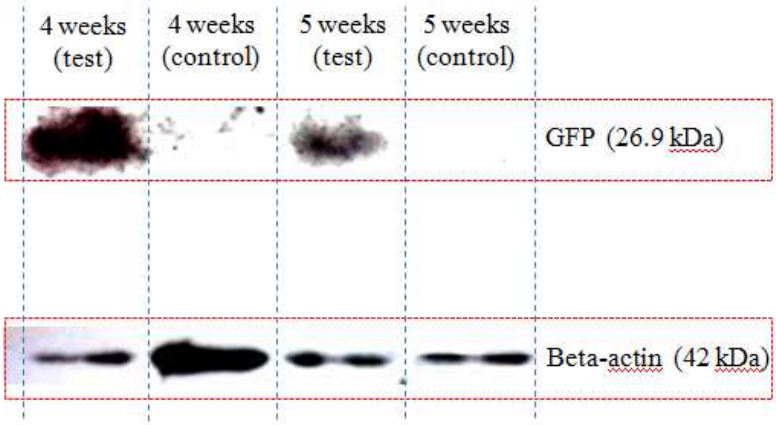

Figure 8. Western blot of both the control (non-pEGFP-loaded) and test (pEGFP-loaded) skin samples from 4- and 5-week-old mice.

Abstract in Korean (국문초록)

의약학 분야에서 나노 수준의 약물이나 유전자를 전달하여 치료하는 방법에 관한 열띤 연구가 진행 되어 왔으며, 특히 나노 수준의 유전자 전달 치료는 수많은 생화학자들로부터 많은 관심을 받아왔다. 유전자 전달 치료의 가능성을 열어준 물질이 유전자 전달 물질이며, 이 물질은 리포좀, 나노 파티클, 유전자-고분자 결합물 등으로 개발 되어 많은 연구가 진행 되어 왔다. 특히 고분자의 경우, 다양한 합성과 변형을 통하여 원하는 기능을 부여할 수 있다는 장점으로 인해 많은 유전자 전달 목적의 고분자 전달체가 개발되었다. 이 고분자 유전자 전달 물질은 바이러스성 벡터와 비교하여 높은 세포 독성을 지닌다는 단점이 있어 많은 개선이 이 이루어 졌으며 그 중에 성공한 하나가 바로 폴리아미도아민(PAMAM) 덴드리머와 그 변형체이다. 낮은 세포 독성으로 확인된 PAMAM의 유전자 전달 효율을 향상시키기 위하여 우리 연구팀에서 이미 연구되고 개발 된 것이 알지닌(R)과 다이에틸트리아민(DETA)으로 변형된, PAMAM-R과 PAM-DET이다.

PAMAM-R는 이미 당뇨병에게 걸린 쥐의 피부 상처를 치료하기 하여 성장인자를 발현할 수 있는 유전자의 전달에 높은 효율을 보이는 것으로 밝혀진 물질이다. 이런 선례에 영감을 받아 나는

경피 흡수를 통한 PAMAM-R를 이용한 동물실험을 시도하였고, 동시에 이는 장차 유전자 치료 차원에서 볼 때 또 다른 적합한 접근 방식이라 생각하였다. 결과적으로는 PAMAM-R G4가 목적 유전자를 무모(hairless) 쥐의 피부조직 중 한 하부조직에 성공적으로 전달한다는 것을 발견하게 되었다.

또한, PAM-DET는 세포막을 뚫고 세포 안으로 진입 후에 엔도좀의 막을 보다 잘 붕괴킬 수 있도록 개발된 유전자 전달체이다. 하지만 이온의 농도가 높은 수용액상태에서 나빠지는 PAM-DET의 폴리플렉스의 안정도는 결국에는 유전자 전달 효율에 나쁜 영향을 끼칠 수 있다. 이에 나는 생체 적합성이 있으면서 소수성인 분자들 중 몇 개를 PAM-DET의 표면에 있는 1차 아민에 결합을 시켜 궁극적으로는 폴리플렉스의 안정도를 향상시키고자 노력하였다. PAM-DET와 소수성 분자 간의 주요 결합방식은 아마이드 혹은 카바마이트 결합을 생성하거나, Traut 시약을 이용한 고리풀림을 이용하여 결합하는 과정을 이용하였다. 폴리 플렉스의 안정도 측정 결과와 유전자 전달 효율 결과를 볼 때, 이렇게 개선된 PAM-DET의 폴리플렉스의 안정도는 친수성 환경에서 대폭 증가하였다.

첫 번째 파트에서는 PAM-DET가 혈액과 같은 높은 이온 강도 조건의 용액 내에서 DNA와 함께 형성하는 폴리플렉스의 안정도를 향상시킬 목적으로 PAM-DET의 표면에 소수성을 띤 그룹인

다이옥시콜레이트 (DC), 다이메틸베타사이클로덱스트린 (DMβCD), 그리고 덱사메타존(DX)을 각각 성공적으로 결합하였다; PAM-DET-DC, PAM-DET- DMβCD, PAM-DET-DX. 각각 합성된 PAM-DET-소수성 그룹 형태의 전달체는 이온 강도를 띠는 수용액 환경에서 폴리플렉스를 형성하였을 때, 동일 조건에서 추가적으로 표면에 합성되지 않은 PAM-DET의 폴리플렉스에 비하여 보다 긴 시간동안 소수성 상호작용으로부터 기인한 크기차원에서의 안성정을 보였으며, HeLa와 U87MG 세포주에서의 유전자 발현 테스트를 해본 결과, 이와 같은 안정성의 영향으로 인하여 유전자 발현 효율이 PAM-DET의 폴리플렉스와 비교하여 향상 되었음을 확인할 수 있었다. 또한 이들 소수성 그룹이 결합된 PAM-DET 물질들의 세포독성은 PAM-DET와 같은 수준임을 확인 할 수 있었다.

두번째 파트에서는 이미 합성이 되어 유전자 전달 효율이 높고, 재현성이 좋은 것으로 입증된 표면이 알지닌으로 둘러쌓여 세포독성이 낮은 PAMAM-R을 생체 조직에 직접적으로 유전자 전달 및 발현을 하기 위한 응용을 시도하였다. 동물의 피부를 구성하고 있는 소기관에 녹색형광단백질 유도유전자(pEGFP)를 PAMAM-R과 함께 폴리플렉스를 이루어 전달 하였고, 그 결과 해당 소기관에서 녹색형광 단백질(GFP)이 발현됨을 형광 이미지와 웨스턴 블랏을 통해 확인하여, 향후 피부조직에 대한 유전자 전달

응용에 대한 가능성을 보게 되었다.

주요어: 유전자전달시스템, 폴리플렉스, PAMAM 덴드리머, PAMAM-R, PAM-DET, 경피전달

학 번: 2004-20482